Supporting Information

Developing strong absorption NIR material through linear planar π-conjugated cyclopalladated complexes dimer

Qi Luo,[a] Jing Zhang,[a] Jiangbin Xia*[a, b]

[a] Hubei Key Lab on Organic and Polymeric Optoelectronic Materials, College of Chemistry and Molecular Sciences, Wuhan University, Wuhan 430072, People's Republic of China

[b] Engineering Research Center of Organosilicon Compounds & Materials, Ministry of Education, College of Chemistry and Molecular Sciences, Wuhan University, Wuhan 430072, P.R. China

jbxia@whu.edu.cn

Table of contents

1. Experimental procedures

1,10-phenanthroline, 3-bromothiophene, 3-(bromomethyl)heptane, $PdCl_2$, boron trifluoride etherate (47%) and [1,3-Bis(diphenylphosphino)propane]dichloronickel(II) ($NiCl_2$(dppp)) were purchased from Adamas-beta without further purification. The other reagents were purchased from the Sinopharm Company. THF was dried by refluxing with sodium and other solvents were used directly. The UV-vis absorption spectra were recorded with a TU-1810 spectrophotometer. The PL spectra were recorded with a NanoLog (Horiba) infrared fluorescence spectrometer. The cyclic voltammetry was performed on CHI750 Electrochemical Workstation. It was carried out in 0.1 M tetrabutylammonium perchlorate/dichloromethane solution, where the concentration of monomers or dimers was 2-3 mg/mL, with glassy carbon electrode as working electrode, platinum wire as counter electrode and Ag/Ag^+ as a reference electrode. All the experiments were performed under N_2 atmosphere at room temperature. The NMR spectra were received using a Bruker 400 MHz spectrometer. The ^1H NMR chemical shifts are referenced to the residual hydrogen signals of the deuterated solvent or TMS, the ^{13}C NMR chemical shifts are referenced to the ^{13}C signals of the deuterated solvent. All spectra were recorded at room temperature unless otherwise noted. The MS (ESI and HRMS) and elemental analysis were performed by the Test Center of Wuhan University. The MALDI-TOF mass spectra were acquired in a Bruker APEX Ⅱ (FT-ICR) high-resolution mass spectrometer with the α-cyano-4-hydroxycinnamic acid as matrix. 1,10-phenanthroline-2-carbaldehyde was prepared according to the reported literature.[1] The $Pd(DMSO)_2Cl_2$ were prepared by heating the solution of $PdCl_2$ (1 g) in DMSO (25 mL) at 50°C until all the $PdCl_2$ dissolved, then the formed yellow precipitates were collected by filtration and washed with Et_2O and acetone before dried under vacuum at room temperature (yield > 95%).

2. Synthesis procedures of ligands and cyclometalated palladium complexes

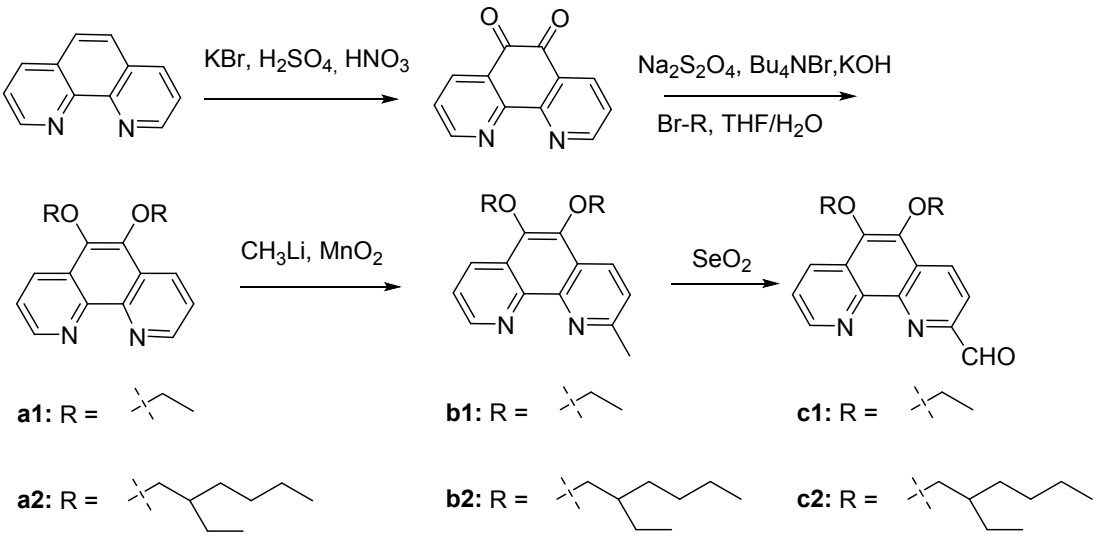

Scheme S1. General procedures for synthesis of 5,6-bis((2-alkoxy)-1,10-phenanthroline-2-carbaldehyde

Synthesis of 1,10-phenanthroline-5,6-dione: The synthesis process is similar to that described in literature.[2] To a mixture of anhydrate phenanthrene (3.0 g, 16.9 mmol), KBr (11.9 g, 0.1 mol) in a Shlenck tube under an ice bath, H_2SO_4 (98%, 40 mL) and HNO_3 (68%, 20 mL) were added subsequently. Then the tube was sealed with Teflon plug and heated for 3 h at 95°C. After cooled to room temperature, the reaction mixture was poured into 1 L water, and the pH was adjusted to 7 with Na_2CO_3. The product was extracted with dichloromethane and dried with anhydrate Na_2SO_4, yellow powder was obtained after the solvent was removed, 3.4 g, 97%.

Synthesis of 5,6-bis(2-alkoxy)-1,10-phenanthroline (a1/a2): The synthesis process of compound **a1/a2** is similar to that described in literature,[2] While the dodecyl bromide was replaced by 3-(bromomethyl)heptane or bromoethane.

a1: Colorless oil (35%). ^{1}H NMR (400 MHz, $CDCl_3$) δ 9.12 (d, *J* = 8 Hz, 2H), 8.58 (d, *J* = 8 Hz, 2H), 7.64 (q, *J* = 4 Hz, 4 Hz, 2H), 4.35 (q, *J* = 6 Hz, 4H), 1.50 (t, *J* = 6 Hz, 6H) ppm; ^{13}C NMR (101 MHz, $CDCl_3$) δ 149.17, 144.25, 142.04, 130.45, 126.43, 122.96, 69.37, 15.85 ppm. In accordance with the reported literature. [3]

a2: Colorless oil (51%). ^{1}H NMR (400 MHz, $CDCl_3$) δ 9.12 (d, *J* = 4 Hz, 2H), 8.57 (d, *J* = 8 Hz, 2H), 8.53 (d, *J* = 8 Hz, 2H), 7.65-7.62 (m, 2H), 4.14-4.10 (m, 4H), 1.89-1.86 (m, 2H), 1.69-1.52 (m, 8H), 1.41-1.36 (m, 8H), 1.02-0.98 (m, 6H), 0.94-0.91 (m, 6H) ppm; ^{13}C NMR (101 MHz, $CDCl_3$) δ 149.10, 144.31, 142.45, 130.28, 126.29, 122.91, 76.79, 40.66, 30.45, 29.15, 23.84, 23.14, 14.14, 11.22 ppm. HRMS (ESI-TOF). Calcd for $C_{28}H_{41}N_2O_2$, $[M+H]^+$ *m/z* 437.3163, found 437.3169.

Synthesis of 5,6-bis((2-alkoxy)-2-methyl-1,10-phenanthroline (b1/b2): To a solution of **a1/a2** (8.57 mmol) in dry THF, CH_3Li (1.6 M, 5.4 mL, 8.57 mmol) was added dropwise at 0°C under nitrogen atmosphere. After stirring overnight at room temperature, water was added and the mixture was extracted with diethyl ether, the organic phase was dried with anhydrate Na_2SO_4. After filtrated, yellowish solution was obtained, active MnO_2 was added and stirred for 3 h. Clean solution was obtained by filtration, the solvent was removed by rotary evaporator. Pure product was obtained as colorless oil by column chromatography on silicone gel

b1: Petroleum ether : ethyl acetate = 1 : 1, 65%. ^{1}H NMR (400 MHz, $CDCl_3$) δ 9.15 (d, *J* = 4 Hz, 1H), 8.59 (d, *J* = 8 Hz, 1H), 8.48 (d, *J* = 8 Hz, 1H), 7.62 (dd, *J* = 4 Hz, 4 Hz, 1H), 7.53 (d, *J* = 8 Hz, 1H), 4.37-4.30 (m, 4H), 1.48-1.52 (m, 6H) ppm; ^{13}C NMR (101 MHz, $CDCl_3$) δ 158.39, 148.89, 143.40, 142.37, 141.15, 130.81, 130.71, 126.47, 124.37, 123.74, 122.68, 69.34, 25.57, 15.84 ppm. HRMS (ESI-TOF). Calcd for $C_{17}H_{19}N_2O_2$, $[M+H]^+$ *m/z* 283.1441, found 283.1447.

b2: Petroleum ether : ethyl acetate = 2 : 1, 60%. ^{1}H NMR (400 MHz, $CDCl_3$) δ 9.12 (d, *J* = 6 Hz, 1H), 8.55 (d, *J* = 8 Hz, 1H), 8.46 (d, *J* = 8 Hz, 1H), 7.61 (m, 1H), 7.52 (d, *J* = 8 Hz, 1H), 4.13-4.07 (m, 4H), 2.93 (s, 3H), 1.90-1.84 (m, 2H), 1.64-1.50 (m, 8H), 1.39-1.35 (m, 8H), 1.01-0.97 (m, 6H), 0.94-0.91 (m, 6H) ppm; ^{13}C NMR (101 MHz, $CDCl_3$) δ 158.22, 149.04, 143.97, 143.80, 142.71, 141.56, 130.59, 130.24, 126.27, 124.15, 123.57, 122.61, 77.26, 40.66, 30.45, 29.15, 25.64, 23.84, 23.14, 14.14, 11.22 ppm. HRMS (ESI-TOF). Calcd for $C_{29}H_{43}N_2O_2$, $[M+H]^+$ *m/z* 451.3319, found 451.3322.

Synthesis of 5,6-bis((2-alkoxy)-1,10-phenanthroline-2-carbaldehyde (c1/c2): A mixture of SeO_2 (0.35 g, 3.1 mmol) and **b1/b2** (3.0 mmol) in dioxane (30 mL) was

reflux at 110°C for 1 h. After cooled to room temperature, clean solution was obtained by filtration and the solvent was removed by rotary evaporator. Pure product was obtained as white solid by column chromatography on silicone gel.

c1: Petroleum ether : ethyl acetate = 2 : 1, 80%. ^{1}H NMR (400 MHz, $CDCl_3$) δ 10.55 (s, 1H, CHO), 9.24 (d, *J* = 4 Hz, 1H), 8.75 (d, *J* = 8 Hz, 1H), 8.68 (d, *J* = 8 Hz, 1H), 8.30 (d, *J* = 8 Hz, 1H), 7.76 (dd, *J* = 4 Hz, 4 Hz, 1H), 4.46-4.32 (m, 4H), 1.55-1.51 (m, 6H) ppm; ^{13}C NMR (101 MHz, $CDCl_3$) δ 194.10, 151.30, 149.69, 144.51, 143.79, 143.64, 141.66, 131.79, 131.29, 129.41, 127.08, 123.57, 119.75, 69.64, 15.79 ppm. HRMS (ESI-TOF). Calcd for $C_{17}H_{17}N_2O_3$, $[M+H]^+$ *m/z* 297.1234, found 297.1238.

c2: Petroleum ether : ethyl acetate = 4 : 1, 75%. ^{1}H NMR (400 MHz, $CDCl_3$) δ 10.54 (s, 1H, CHO), 9.22 (d, *J* = 4 Hz, 1H), 8.72 (d, *J* = 8 Hz, 1H), 8.64 (d, *J* = 8 Hz, 1H), 8.30 (d, *J* = 8 Hz, 1H), 7.74-7.71 (m, 1H), 4.23-4.09 (m, 4H), 1.93-1.87 (m, 2H), 1.66-1.48 (m, 8H), 1.41-1.34 (m, 8H), 1.02-0.95 (m, 6H), 0.94-0.91 (m, 6H) ppm; ^{13}C NMR (101 MHz, $CDCl_3$) δ 194.17, 151.19, 149.86, 145.05, 144.17, 143.92, 141.92, 131.57, 130.82, 129.25, 126.88, 123.52, 119.65, 76.93, 40.66, 40.63, 30.42, 30.40, 29.12, 23.83, 23.82, 23.12, 14.13, 11.20 ppm. HRMS (ESI-TOF). Calcd for $C_{29}H_{41}N_2O_3$, $[M+H]^+$ *m/z* 465.3112, found 465.3117.

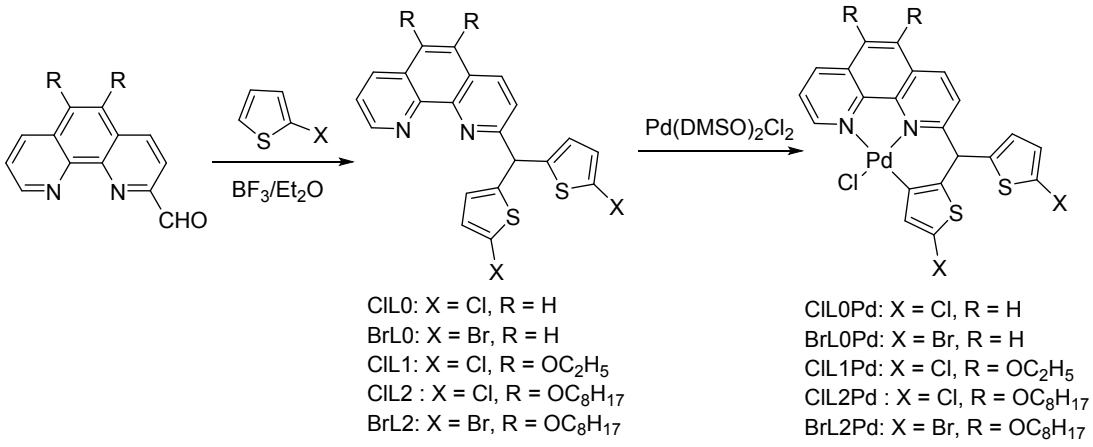

Scheme S2. General procedures for synthesis of ligand and cyclometalated palladium complexes

General procedures for synthesis of XLn (X = Cl or Br, n = 0, 1, 2): Thiophene (4 mmol) and phenanthroline-2-carbaldehyde (1 mmol) were dissolved in glacial acetic acid (6 mL), 3 mL BF_3/Et_2O (47%) was added and stirred for 2 h at 50°C. The mixture was poured into 50 mL water and then extracted with ethyl acetate. The organic phase was washed with saturated sodium carbonate solution and the solvent was removed under vacuum. Pure product was obtained by column chromatography on silicone gel (petroleum : ethyl acetate = 4 : 1).

ClL0: White solid, 63%. ^{1}H NMR (400 MHz, DMSO-D_6) δ 9.21 (d, *J* = 4 Hz, 1H), 8.53-8.50 (m, 2H), 8.01 (s, 2H), 7.88 (d, *J* = 8 Hz, 1H), 7.81-7.78 (m, 1H), 6.95-6.97 (m, 4H), 6.44 (s, 1H, CH) ppm; ^{13}C NMR (101 MHz, DMSO-D_6) δ 160.56, 151.37, 146.20, 146.15, 145.59, 138.93, 137.21, 129.81, 129.21, 128.45, 127.93, 127.33, 127.03, 126.83, 124.51, 123.48, 50.57 ppm. HRMS (ESI-TOF). Calcd for $C_{21}H_{13}Cl_2N_2S_2$, $[M+H]^+$ *m/z* 426.9892, found 426.9895.

BrL0: Lightly green solid, 47%. ^{1}H NMR (400 MHz, $CDCl_3$) δ 9.31 (d, *J* = 4 Hz, 1H), 8.41 (d, *J* = 8 Hz, 1H), 8.29 (d, *J* = 8 Hz, 1H), 7.86 (s, 1H), 7.72-7.76 (m, 2H), 6.89 (d, *J* = 4 Hz, 1H), 6.72 (d, *J* = 4 Hz, 1H), 6.40 (s, 1H, CH) ppm; ^{13}C NMR (101 MHz, $CDCl_3$) δ 161.54, 146.29, 137.96, 137.44, 129.64, 129.23, 127.98, 127.26, 126.92, 126.61, 123.35, 122.71, 112.03, 51.46 ppm. In accordance with our previously reported literature.[4]

ClL1: White solid, 89%. ^{1}H NMR (400 MHz, $CDCl_3$) 9.19 (d, *J* = 4 Hz, 1H), 8.59-8.62 (m, 2H), 7.70 (d, *J* = 8 Hz, 1H), 7.66 (dd, *J* = 4 Hz, 4 Hz, 1H), 6.76 (d, *J* = 4 Hz, 2H), 6.72 (m, 2H), 6.39 (s, 1H, CH), 4.31-4.36 (m, 4H), 1.47-1.52 (m, 6H) ppm; ^{13}C NMR (101 MHz, $CDCl_3$) δ 159.98, 149.24, 143.86, 142.17, 142.11, 131.90, 130.90, 129.70, 126.94, 126.04, 125.78, 125.69, 123.01, 122.11, 69.44, 51.40, 15.85 ppm. HRMS (ESI-TOF). Calcd for $C_{25}H_{21}Cl_2N_2O_2S_2$, $[M+H]^+$ *m/z* 515.0416, found 515.0419.

ClL2: Brown oil, 91%. ^{1}H NMR (400 MHz, $CDCl_3$) δ 9.17 (d, *J* = 6 Hz, 1H), 8.60-8.57 (m, 2H), 7.70 (d, *J* = 8 Hz, 1H), 7.66-7.62 (m, 1H), 6.76 (d, *J* = 4 Hz, 2H), 6.71 (d, *J* = 4 Hz, 2H), 6.39 (s, 1H), 4.12-4.09 (m, 4H), 1.88-1.85 (m, 2H), 1.64-1.52 (m, 8H), 1.42-1.33 (m, 8H), 1.01-0.97 (m, 6H), 0.94-0.91 (m, 6H) ppm; ^{13}C NMR (101 MHz, $CDCl_3$) δ 159.83, 149.39, 143.95, 142.67, 142.38, 131.72, 130.48, 129.69, 126.75, 126.02,

125.77, 125.53, 122.93, 121.99, 76.92, 76.82, 51.42, 40.65, 30.45, 29.17, 29.15, 23.83, 23.14, 14.15, 11.24, 11.22 ppm. HRMS (ESI-TOF). Calcd for $C_{37}H_{45}Cl_2N_2O_2S_2$, $[M+H]^+$ *m/z* 683.2294, found 683.2291.

BrL2: Brown oil, 88%. ^{1}H NMR (400 MHz, $CDCl_3$) δ 9.18 (d, *J* = 4 Hz, 1H), 8.60-8.57 (m, 2H), 7.70 (d, J = 8 Hz, 1H), 7.67-7.63 (m, 1H), 6.90 (d, *J* = 4 Hz, 2H), 6.71 (d, *J* = 4 Hz, 2H), 6.43 (s, 1H), 4.13-4.09 (m, 4H), 1.88-1.84 (m, 2H), 1.64-1.49 (m, 8H), 1.38-1.35 (m, 8H), 1.01-0.97 (m, 6H), 0.94-0.90 (m, 6H) ppm; ^{13}C NMR (101 MHz, $CDCl_3$) δ 159.32, 148.41, 146.90, 145.00, 143.14, 142.80, 142.78, 135.86, 133.11, 132.38, 132.22, 129.41, 127.06, 126.94, 126.49, 125.68, 125.52, 125.45, 124.49, 121.63, 77.49, 77.35, 53.17, 40.56, 30.33, 29.06, 23.75, 23.08, 23.07, 14.11, 14.10, 11.20, 11.15 ppm. HRMS (ESI-TOF). Calcd for $C_{37}H_{45}Br_2O_2N_2S_2$, $[M+H]^+$ *m/z* 773.1263, found 773.1267.

General procedures for synthesis of cyclometalated palladium complexes XLnPd (X = Cl or Br, n = 0, 1, 2): To a mixture of $Pd(DMSO)_2Cl_2$ (0.5 mmol) in 30 mL CH_3OH, ligand (0.5 mmol) dissolved in a mixture of CH_2Cl_2/CH_3OH (2 mL/10 mL) was added dropwise under strong stirring. The mixture was stirred at room temperature overnight, the generated precipitates were collected by filtration and dried under vacuum. All the synthesized cyclopalladated monomers are stable in solid state, neat dichloromethane and chloroform.

ClL0Pd: Lightly green solid, 89%. ^{1}H NMR (400 MHz, DMSO-D_6) δ 9.36 (d, *J* = 4 Hz, 1H), 8.92-8.88 (m, 2H), 8.31 (d, *J* = 4 Hz, 1H), 8.26-8.15 (m, 3H), 7.33 (d, *J* = 4 Hz, 1H), 7.05 (d, *J* = 4 Hz, 1H), 6.86 (d, *J* = 4 Hz, 1H), 6.81 (s, 1H, CH) ppm; The ^{13}C NMR of **ClL0Pd** was unavailable for it's bad solubility and unstable property in DMSO. Elemental analysis (calcd. for $C_{21}H_{11}Cl_3N_2S_2Pd$): C (44.39, 44.57), H (1.95, 2.06), N (4.93, 4.81); HRMS (ESI-TOF). Calcd for $C_{21}H_{12}Cl_3N_2S_2Pd$, $[M+H]^+$ *m/z* 566.8537, found 566.8540.

BrL0Pd: Pale yellow, 85%. ^{1}H NMR (400 MHz, CD_2Cl_2) δ 9.50 (d, *J* = 4 Hz, 1H), 8.50-8.54 (m, 4H), 7.87-7.97 (m, 4H), 7.56 (s, 1H), 6.82 (d, *J* = 4 Hz, 1H), 6.77 (d, *J* = 4 Hz, 1H), 6.19 (s, 1H, CH) ppm. The ^{13}C NMR of **BrL0Pd** was unavailable for its bad solubility in CD_2Cl_2. Elemental analysis (calcd. for $C_{21}H_{11}ClBr_2N_2S_2Pd$: C (38.38, 38.51),

H (1.69, 1.65), N (4.26, 4.33); HRMS (ESI-TOF). Calcd for $C_{21}H_{12}ClBr_2N_2S_2Pd$, $[M+H]^+$ *m/z* 658.7591, found 658.7596.

ClL1Pd: Lightly green solid, 86%. ^1H NMR (400 MHz, $CDCl_3$) δ 9.20 (d, *J* = 4 Hz, 1H), 8.73 (d, *J* = 8 Hz, 1H), 8.66 (d, *J* = 8 Hz, 1H), 7.83 (d, *J* = 8 Hz, 1H), 7.70 (dd, *J* = 4 Hz, 4 Hz, 1H), 7.37 (s, 1H), 6.80 (d, *J* = 4 Hz, 1H), 6.72 (d, *J* = 4 Hz, 1H), 6.13 (s, 1H), 4.49-4.371 (m, 4H), 1.58-1.51 (m, 6H) ppm; ^{13}C NMR (101 MHz, $CDCl_3$) δ 157.52, 148.11, 147.98, 144.78, 142.79, 142.74, 142.70, 138.04, 133.67, 132.82, 132.52, 131.23, 129.57, 127.32, 127.12, 125.86, 125.77, 124.21, 112.83, 107.19, 70.27, 70.02, 53.46, 15.90, 15.85 ppm. Elemental analysis (calcd. for $C_{25}H_{19}Cl_3N_2O_2S_2Pd$): C (45.75, 45.98), H (2.92, 2.88), N (4.27, 4.35); HRMS (ESI-TOF). Calcd for $C_{25}H_{20}Cl_3N_2O_2S_2Pd$, $[M+H]^+$ *m/z* 654.9061, found 654.9068.

ClL2Pd: Lightly green solid, 86%. ^1H NMR (400 MHz, $CDCl_3$) δ 9.34 (d, *J* = 4 Hz, 1H), 8.72 (d, *J* = 8 Hz, 1H), 8.68 (d, *J* = 8 Hz, 1H), 7.86 (d, *J* = 8 Hz, 1H), 7.78 (m, 1H), 7.29 (s, 1H), 6.84 (d, *J* = 4 Hz, 1H), 6.60 (d, *J* = 4 Hz, 1H), 6.15 (s, 1H), 4.23-4.11 (m, 4H), 1.91-1.86 (m, 2H), 1.64-1.53 (m, 8H), 1.38-1.35 (m, 8H), 1.01-0.91 (m, 6H), 0.94-0.91 (m, 6H) ppm; ^{13}C NMR (101 MHz, $CDCl_3$) δ 57.60, 148.24, 145.31, 144.96, 143.36, 142.93, 142.85, 134.45, 133.40, 132.42, 132.11, 130.54, 128.08, 127.27, 126.90, 125.83, 125.58, 124.78, 124.65, 124.40, 77.61, 77.27, 53.64, 40.60, 30.37, 29.11, 23.77, 23.11, 14.14, 11.20 ppm. Elemental analysis (calcd. for $C_{37}H_{43}Cl_3N_2O_2S_2Pd$): C (53.89, 54.15), H (5.26, 5.38), N (3.40, 3.31). HRMS (ESI-TOF). Calcd for $C_{37}H_{44}Cl_3N_2O_2S_2Pd$, $[M+H]^+$ *m/z* 823.0939, found 823.0943.

BrL2Pd: Lightly green solid, 88%. ^1H NMR (400 MHz, $CDCl_3$) δ 9.34 (d, *J* = 4 Hz, 1H), 8.72 (d, *J* = 8 Hz, 1H), 8.68 (d, J = 8 Hz, 1H), 7.86 (d, J = 8 Hz, 1H), 7.78 (m, 1H), 7.29 (s, 1H), 6.84 (d, J = 4 Hz, 1H), 6.60 (d, *J* = 4 Hz, 1H), 6.15 (s, 1H), 4.23-4.11 (m, 4H), 1.91-1.86 (m, 2H), 1.64-1.53 (m, 8H), 1.38-1.35 (m, 8H), 1.01-0.91 (m, 6H), 0.94-0.91 (m, 6H) ppm; ^{13}C NMR (101 MHz, $CDCl_3$) δ 157.50, 148.08, 144.92, 143.35, 142.99, 142.86, 138.05, 133.41, 132.95, 132.37, 131.12, 129.58, 127.24, 126.98, 125.79, 125.71, 124.28, 112.85, 107.20, 77.63, 77.25, 53.49, 40.61, 30.37, 29.12, 23.78, 23.12, 14.15, 11.22 ppm. Elemental analysis (calcd. for $C_{37}H_{43}ClBr_2N_2O_2S_2Pd$): C

(48.65, 48.81), H (4.74, 4.65), N (3.07, 2.94); HRMS (ESI-TOF). Calcd for $C_{37}H_{44}ClBr_2N_2O_2S_2Pd$, $[M+H]^+$ *m/z* 912.9908, found 912.9912.

General procedures for preparing $(XL2Pd)_2$ (X = Cl or Br): The monomer (0.3 mmol) was dissolved in DMF (5 mL) and settled down for a night, dark precipitates generated and anhydrate ethyl ether (5 mL) was added. Most of the red **$(XL2Pd)_2$** are big solid and quickly sink to the bottom while the white dimethylamine salts are small crystals and suspended in the solvent. The solution poured and the precipitate washed with 4 x 10 mL ethyl ether and dried under vacuum to give the **$(XL2Pd)_2$**. The products appear wine red when settling in the organic solvent and appear dark in the normal state (the pictures of **$(BrL2Pd)_2$** showed in Figure S1). The dimethylamine salt was isolated as white solid, and the NMR spectra showed in Figure S2.

$(ClL2Pd)_2$: Dark solid, 83%. ^{1}H NMR (400 MHz, $CDCl_3$) δ 9.81 (s, 2H), 8.80 (2H), 8.43 (2H), 8.04 (2H), 7.68 (2H), 7.51 (2H), 7.03 (2H), 6.81 (2H), 4.0-4.10 (8H), 1.81 (4H), 1.19-1.59 (m, 24H), 0.87-0.94 (m, 16 H), 0.68 (m, 8H) ppm; Elemental analysis (calcd. for $C_{74}H_{84}Cl_4N_4O_4S_4Pd_2$): C (56.38, 56.51), H (5.37, 5.44), N (3.55, 3.62); HRMS (m/z): $[M-2Cl^-+2CF_3COO^-+CH_3OH+H^++Na^+]^{2+}$, 893.1435; found, 893.1426.

$(BrL2Pd)_2$: Dark solid, 87%. ^{1}H NMR (400 MHz, $CDCl_3$) δ 10.02-9.79 (br, 2H), 8.78 (2H), 8.40 (2H), 8.02 (2H), 7.65 (2H), 7.45 (2H), 7.13 (2H), 6.73 (2H), 4.0-4.10 (8H), 1.81 (4H), 1.19-1.59 (m, 24H), 0.87-0.94 (m, 16 H), 0.68 (m, 8H) ppm. MALDI-TOF : *m/z* found 1630.113 $[M-Cl]^+$; 1665.464 $[M+H]^+$; 1710.246 $[M-Cl+Br+H]^+$. Elemental analysis (calcd. for $C_{74}H_{84}Cl_2Br_2N_4O_4S_4Pd_2$): C (53.37, 52.44), H (5.08, 4.77), N (3.36, 3.19), the relatively big deviation are ascribed to the partially replaced Cl^- by Br^-, which was demonstrated by the MALDI-TOF data.

3. Results and Discussion

Characterization of dimer

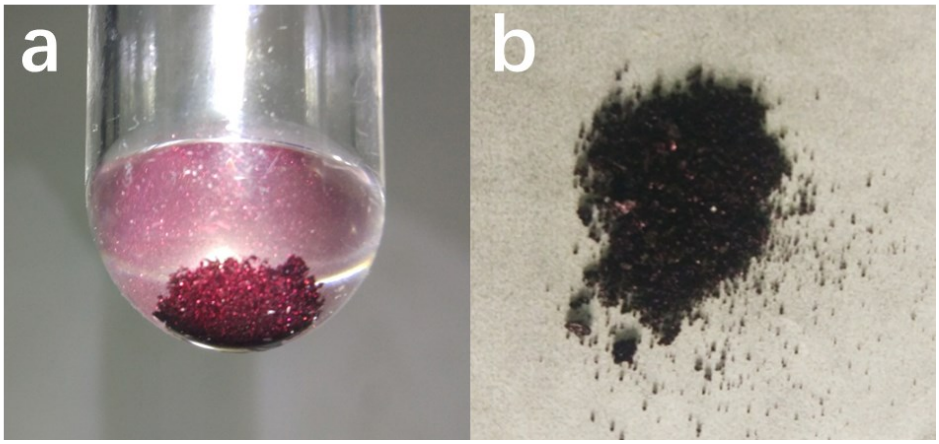

Figure S1. Pictures of **$(BrL2Pd)_2$**: (a) Settled in diethyl ether; (b) In normal state.

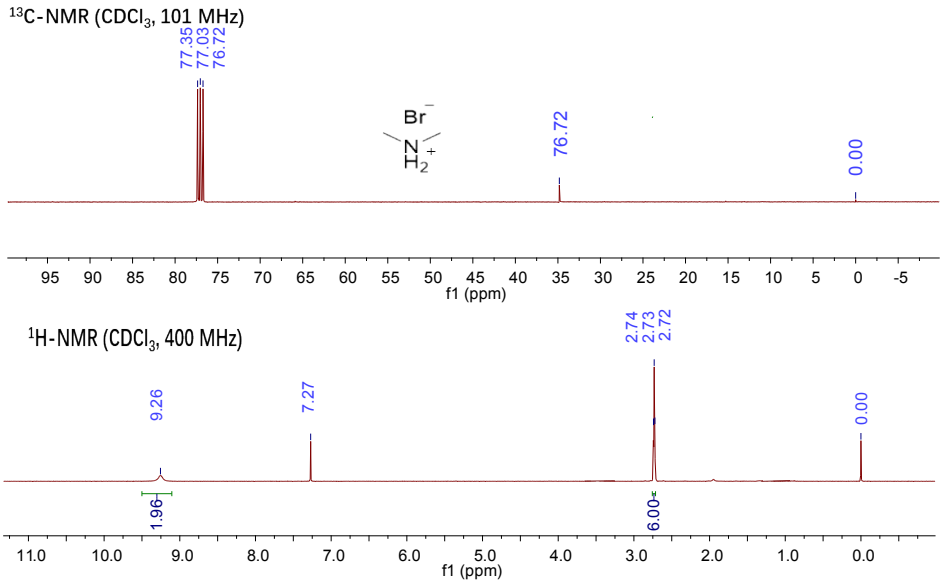

Figure S2. ^{1}H NMR and ^{13}C NMR spectra of dimethylamine bromide.

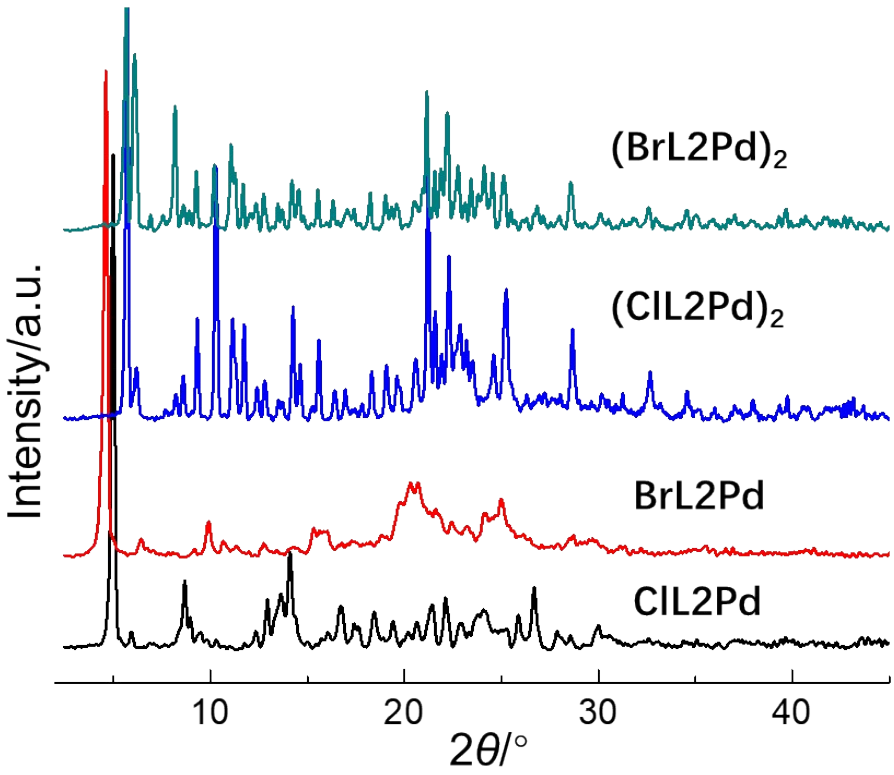

Figure S3. X-ray diffraction (XRD) patternS of **ClL2Pd**, **BrL2Pd**, **$(ClL2Pd)_2$** and **$(BrL2Pd)_2$**. The intense sharp peaks in X-ray diffraction pattern show that these dimers have a good crystalline morphology, indicating there is strong intermolecular interaction between dimers.

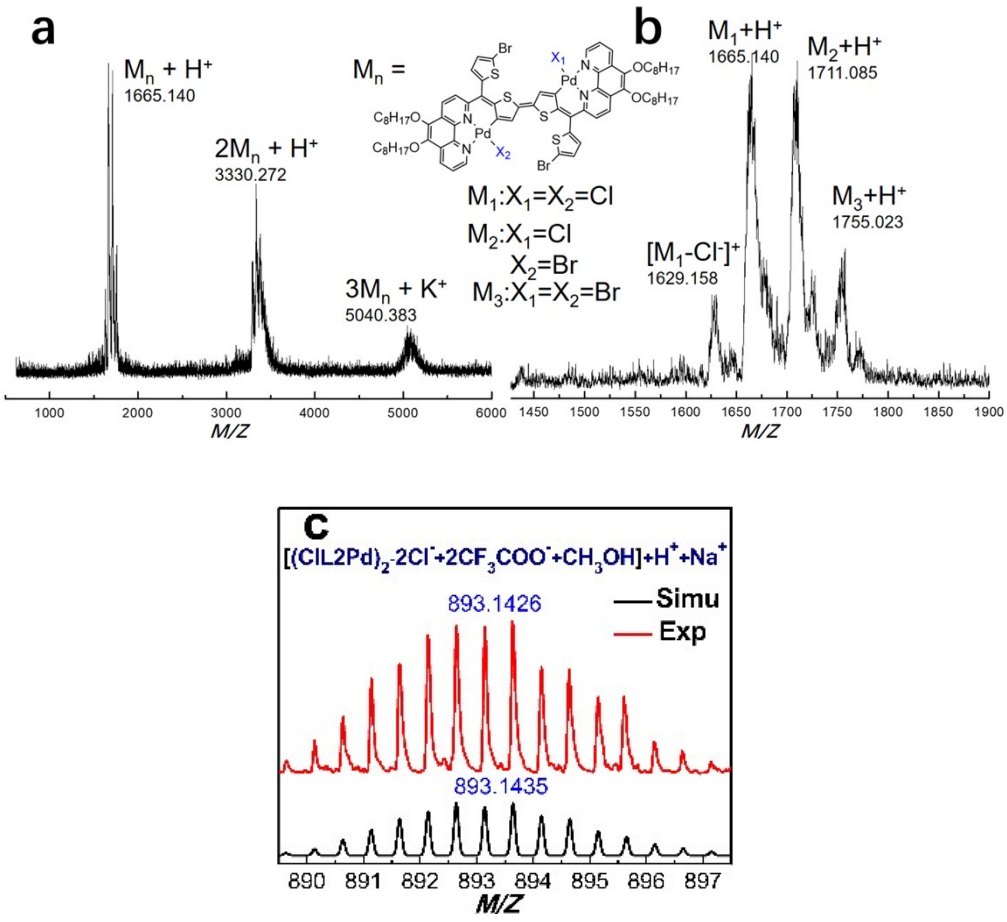

Figure S4. The MALDI-TOF mass spectra of **$(BrL2Pd)_2$**: (a) Full spectra and (b) enlarged spectra, where the M1, M2 and M3 represent for different halogen (Cl^- or Br^-) coordinated dimers. (c) HRMS spectra of **$(ClL2Pd)_2$-$2Cl^-$+$2CF_3COO^-$ +CH_3OH]+H^++Na^+**:simulative (black) and experimental (red) curves.

In the MALDI-TOF mass spectra of dimer **$(BrL2Pd)_2$**, besides the signals of dimers around 1665.140, the signals of di-dimers (3330.272 for $[2M+H]^+$) and tri-dimers (5040.383 for $[3M+K]^+$) were also observed, which is ascribed to the strong intermolecular effect such as π-π interaction between dimers. Meanwhile, the Cl^- coordinated to the Pd could be replaced by Br^- (1711.085, 1755.023 in Figure S4b) in this step. The HRMS spectra of **$(ClL2Pd)_2$** showed in Figure S4c also reveals the formation of dimer (893.1426 for 2+ ions).

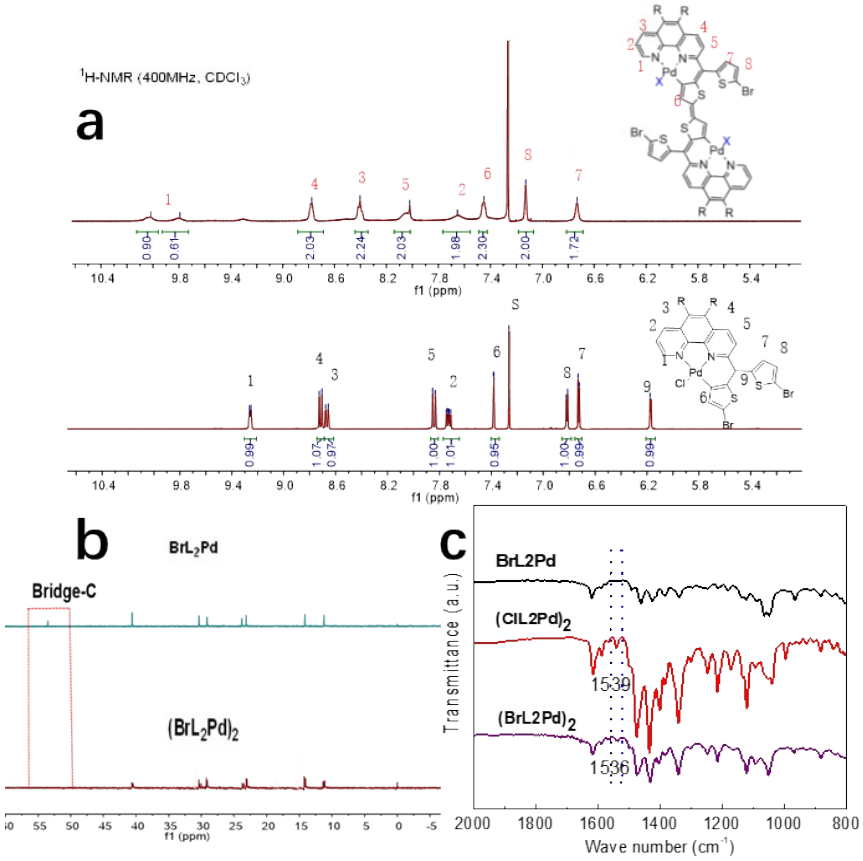

Figure S5. (a) ^{1}H NMR spectra of **BrL2Pd** and **$(BrL2Pd)_2$**; (b) High field ^{13}C-NMR spectra of **BrL2Pd** and **$(BrL2Pd)_2$**; (c) FT-IR spectra of **BrL2Pd**, **$(ClL2Pd)_2$** and **$(BrL2Pd)_2$**. (The proton signals of the **$(BrL2Pd)_2$** appear as broad peaks and the signals of N=C-H are divided into two parts, 9.79 and 10.02 ppm, respectively, which can be ascribed to the isomers with different halogen atoms (9.79 ppm for Cl and 10.02 ppm for Br) and could not be observed in **$(ClL2Pd)_2$** (Figure S41))

The signal of the tertiary hydrogen in **$(BrL2Pd)_2$** disappears while it appears at 6.18 ppm in **BrL2Pd** (marked as 9). Meanwhile, the signal of the triaryl-carbon in **$(BrL2Pd)_2$** is absent while it appears at 53.49 ppm in **BrL2Pd** (marked as Bridge-C). Both results demonstrate the formation of QTM structure. The proton signals of aromatic thiophenes appear at the relatively high field of 6.73 and 7.13 ppm (Figure S5a, marked as 7 and 8) while that of the quinoid thiophenes locate at 7.45 ppm (marked as 6), and all the phenanthroline hydrogen signals appear at the region of 7.65-10.02 ppm.

Mechanism study

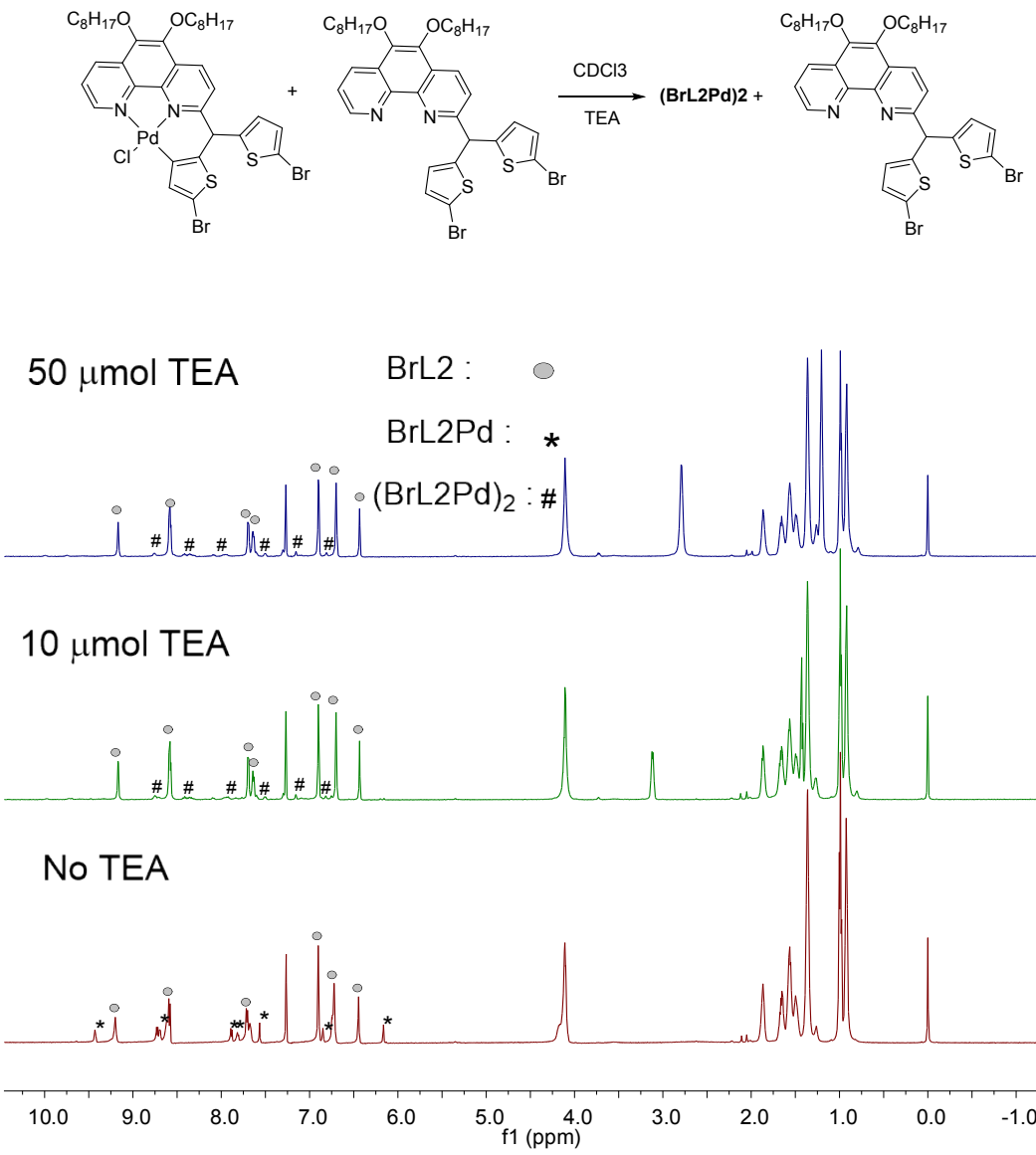

Figure S6. ^{1}H NMR traces of the reaction between **BrL2** and **BrL2Pd** in the presence of TEA. (3 μmol **BrL2Pd** and 7 μmol **BrL2**)

The mechanism of the dimerization was studied. From the structure of the dimers, the dimerization only occurs between the Pd-coordinated thiophene. In addition, when triethylamine was added to the mixed solution of **BrL2** and **BrL2Pd** (3 μmol : 7 μmol) in $CDCl_3$ and after which the ^{1}H NMR was recorded, only the complexes was reacted while the ligand **BrL2** remained unchanged (Figure S6). Other halogen-

substituted thiophene derivatives were used to replace the **BrL2** and result in the same phenomenon. These results reveal that the six-membered ring consisting of Pd, N and C is crucial in the dimerization process. Thus, the possible dimerization mechanism was proposed in Scheme S3. At first, the triaryl-carbanion species **a** was formed in the presence of the base (such as DMF or TEA), in which the six-membered ring structure facilitated the progress. The species **a** would change to another anion species **b** which has quinoid thiophene structure and terminal carbanion. The electrophilic addition between the species **b** and monomer results in the intermediate species **c**, which could form anion species **d** through the elimination of X_2 (Br_2 or Cl_2). The species **d** would be oxidized by the generated X_2, resulting in the formation of quinoid dimers.

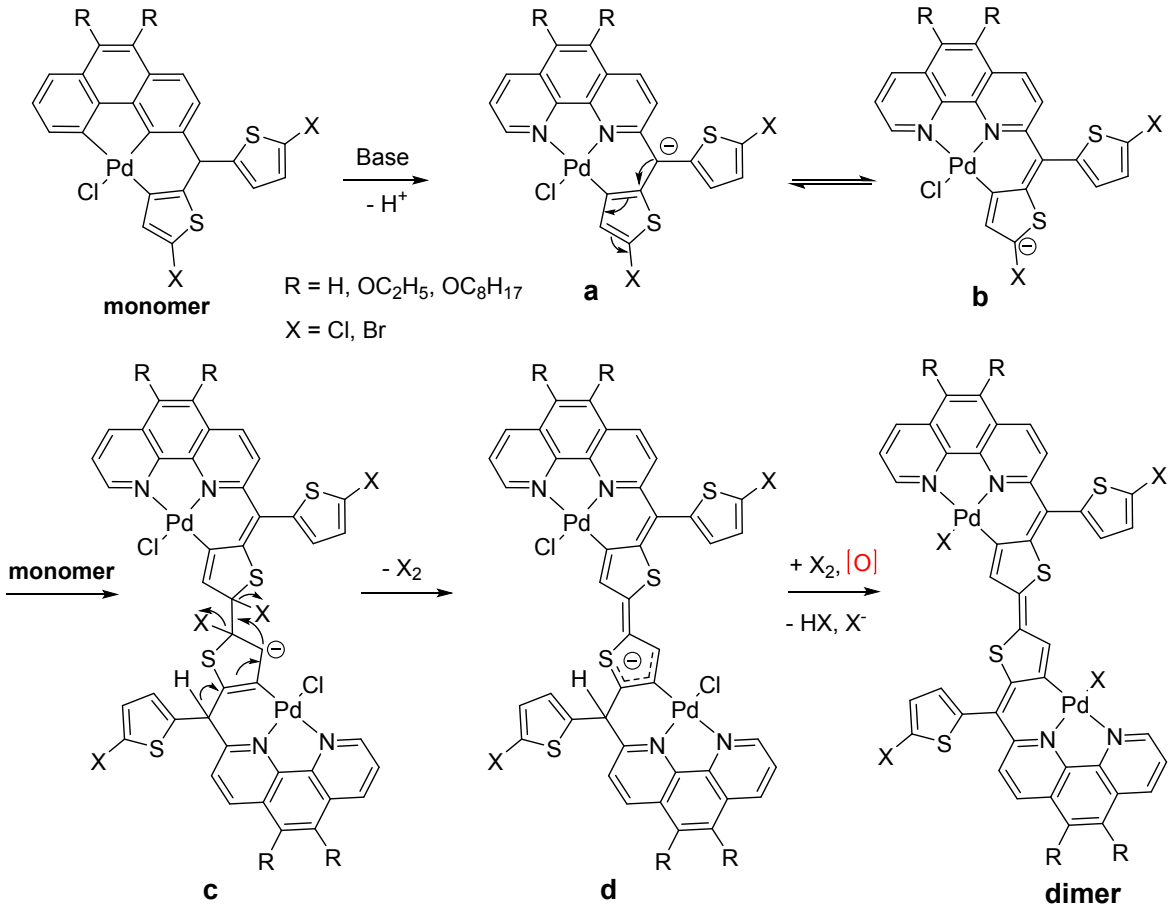

Scheme S3. Proposed mechanism of the dimerization process.

Experimental details of calculating the fluorescence quantum yields:

The fluorescence quantum yields were evaluated by the relative comparison measurement with the following equations:

$$\phi = \phi_s \frac{IA_s}{I_s A}\left(\frac{n}{n_s}\right)^2 \qquad I = \int_{\lambda_1}^{\lambda_2} I_{f,\lambda}\, d(\lambda)$$

Where the ϕ and A are the fluorescence quantum yields and absorption value, respectively. The *I* is the integral area of the emission spectrum with the λ_1 and λ_2 as the starting and ending wavelength of the emission peak. The *n* represents the refractive index of solvent and the *s* represents the standard fluorescence compound. The indocyanine green (ICG) was chosen as the standard fluorescence compound with the fluorescence quantum yields of 0.13 in DMSO when excited at 650 nm. The absorption value is no more than 0.05, and the emission spectrum collected with the exciting laser of 650 nm. The n is 1.4244 in dichloromethane and n_s is 1.47976 in DMSO. The I-A graphic was shown in Figure S7 and the fluorescence quantum yield of **(BrL2Pd)$_2$** is calculated to be 0.036.

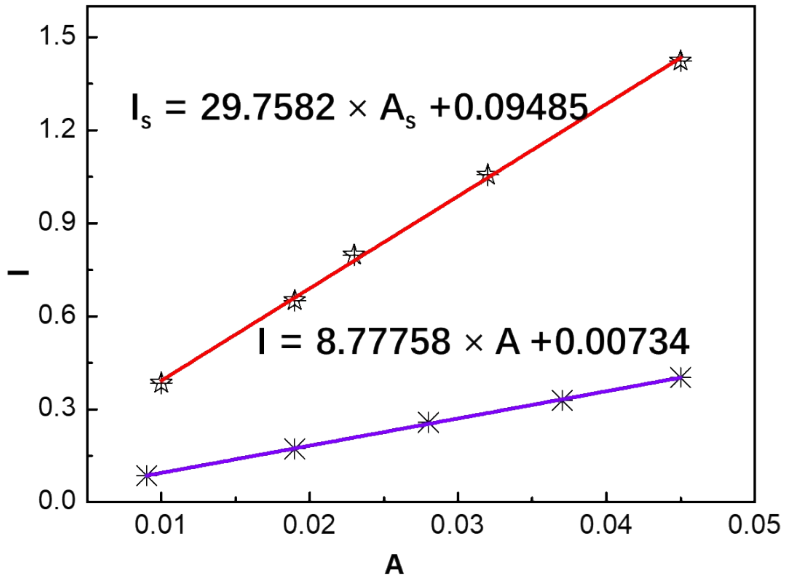

Figure S7. The I-A graphic of ICG and **(BrL2Pd)$_2$**.

Optical Spectra

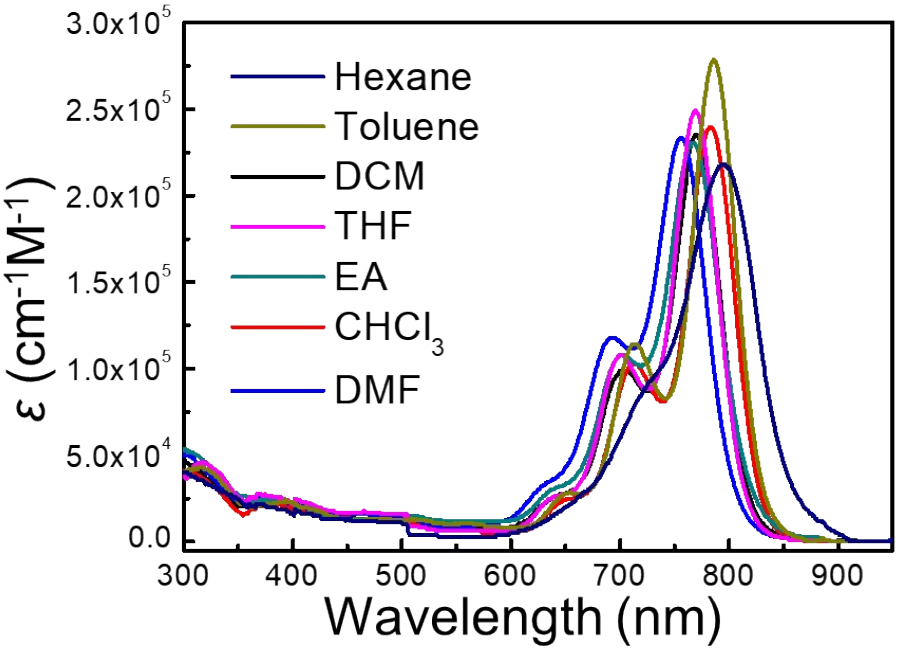

Figure S8. Absorption coefficients of **$(BrL2Pd)_2$** in different solvent.

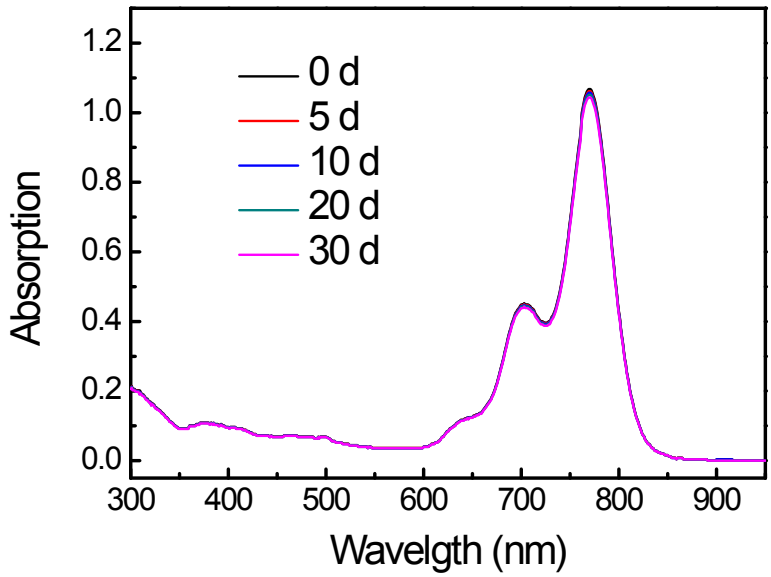

Figure S9 Stability of **$(BrL2Pd)_2$** in DCM evaluated by monitoring the absorption spectra as a function of time. The DCM solution containing **$(BrL2Pd)_2$** was sealed in a brown bottle and allowed to stand under room temperature. The absorption was monitored every 5 d or 10 d over a total monitoring time of 30 d.

Cyclic voltammetry:

The cyclic voltammograms were acquired in dichloromethane with the tetrabutylammonium perchlorate (TBAP) as supporting electrolyte, glassy carbon electrode as working electrode, platinum wires as counter electrode and Ag/Ag^+ as a reference electrode. All the experiments were performed under N_2 atmosphere at room temperature. The electrochemical potential of Ag/Ag^+ was calibrated with respect to the ferrocene/ferrocenium (Fc/Fc^+) couple. The half-wave potential ($E_{1/2}$) of Fc/Fc^+ measured in 0.1 M TBAP dichloromethane solution is 0.04 V vs. Ag/Ag^+ and the orbital energy of ferrocene uses -4.80 eV as reference.[5] Thus, the electrode potential for the Ag/Ag^+ was assumed to be −4.76 eV and the energy level of the materials could be acquired using the following equation: E^{LUMO} (eV) = -4.76- E^{onset}_{red} V. The HOMOs were estimated from the LUMOs energy level and E_g, where E_g is the optical bandgap.

Table S1. Detailed electrochemical and optical properties of **BrL2Pd**, **$(ClL2Pd)_2$** and **$(BrL2Pd)_2$**.

	E^{onset}_{red}/V[a]	LUMO/eV[b]	λ_{max}/nm	λ_{onset}/nm	E_g/eV[c]	HOMO/eV[d]
BrL2Pd	-1.55	-3.21	337	489	2.54	-5.75
$(ClL2Pd)_2$	-0.81	-3.95	769	849	1.46	-5.41
$(BrL2Pd)_2$	-0.84	-3.92	771	849	1.46	-5.38

[a] In V vs Ag/Ag^+. All the potentials were calibrated with Fc/Fc^+ (E1/2 = +0.04 V measured under identical condition).

[b] Estimated with the following equation: E^{LUMO} (eV) = -4.76- E^{onset}_{red}.

[c] Calculated from the relation: E_g (eV)= $1240/\lambda_{onset}$.

[d] Estimated from the LUMO energy level and E_g.

Photocurrent responses experiments:

The dimers **(ClL2Pd)$_2$** and **(BrL2Pd)$_2$** were dissolved in DCM with the concentration of 2 mg/mL, 50 μL of the above solution was adding slowly to a 1 cm × 1 cm ITO glass. After all the organic solvent was evaporated, the ITO was covered with green film and was used as a working electrode. The photocurrent was acquired in 0.1 M KCl under 0.2 V bias voltage with the platinum wires as a counter electrode and calomel as a reference electrode. The irradiation light was from a 300 W Xe lamp (PLS-SXE300) with a filter (> 600 nm), and the experiment was performed in the night without any other light except the light from the lamp.

Crystal data

Single crystals of **BrL0Pd** suitable for X-ray diffraction analysis were obtained as lightly green prism by slow evaporation of the complexes solution in DCM. However, for the poor solubility of the dimer **(ClL1Pd)$_2$**, the single crystals were grown in situ. Dark brown stick crystals were acquired by putting the solution of the monomer **ClL1Pd** in the mixture of DCM/DMF (6 mg/20 mL/0.2 mL) for weeks. The monomer **BrL0Pd** displays a distorted planar quadrilateral geometry around the metal center, which has a five-membered ring (Pd1, N1, C14, C15, N2) and a six-membered ring (Pd1, C3, C4, C5, C10, N1) in the coordinated structure. Selected bond lengths and angles of monomer and dimer were listed in Table S2 and Table S3, respectively.

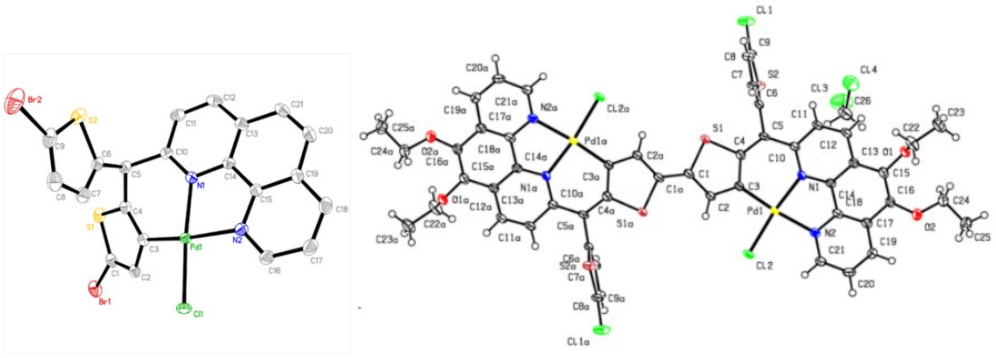

Table S2. Selected bond lengths (Å) and angles (deg) of **BrL0Pd**.

Pd(1)-N(1)	2.034(2)	C(5)-C(6)	1.524(4)	N(2)-Pd(1)-Cl(1)	94.16(7)
Pd(1)-N(2)	2.110(2)	C(5)-C(10)	1.515(4)	C(4)-C(3)-Pd(1)	121.0(2)
Pd(1)-Cl(1)	2.2974(7)	N(1)-C(10)	1.337(4)	C(3)-C(4)-C(5)	128.4(3)
Pd(1)-C(3)	1.981(3)	C(3)-Pd(1)-N(1)	91.58(11)	C(4)-C(5)-C(10)	112.6(2)
C(3)-C(2)	1.431(4)	C(3)-Pd(1)-N(2)	167.95(10)	N(1)-C(10)-C(5)	118.8(2)
C(4)-C(3)	1.358(4)	N(1)-Pd(1)-N(2)	80.79(9)	C(10)-C(5)-C(4)-C(3)	46.9(4)
C(4)-C(5)	1.502(4)	C(3)-Pd(1)-Cl(1)	93.33(9)	N(1)-C(10)-C(5)-C(4)	-44.3(3)
C(7)-C(6)	1.350(4)	N(1)-Pd(1)-Cl(1)	174.93(7)		

Table S3. Selected bond lengths (Å) and angles (deg) of **(ClL1Pd)$_2$**.

PD1-C(3)	1.970(4)	C(5)-C(4)	1.365(5)	C(10)-N(1)-PD1	128.9(2)
PD1-N(1)	2.030(3)	C(5)-C(6)	1.493(5)	C(4)-C(5)-C(10)	124.3(3)
PD1-N(2)	2.097(3)	C(5)-C(10)	1.460(5)	C(1)#1-C(1)-C(2)	127.5(4)
PD1-Cl2	2.3218(9)	C(3)-PD1-N(1)	92.95(14)	C(2)-C(1)-S(1)-C(4)	1.9(3)
C(1)-C(1)a	1.395(7)	C(3)-PD1-N(2)	173.87(13)	S(1)-C(1)-C(2)-C(3)	-0.9(4)
C(1)-C(2)	1.404(5)	N(1)-PD1-N(2)	81.38(12)	C(1)-S(1)-C(4)-C(3)	-2.4(3)
C(2)-C(3)	1.380(5)	C(3)-PD1-CL2	93.36(11)	C(1)-C(2)-C(3)-C(4)	-0.9(5)
C(4)-C(3)	1.441(5)	N(1)-PD1-CL2	172.94(9)	S(1)-C(4)-C(3)-C(2)	2.3(4)

Table S4. Crystal data and structure refinement for **BrL0·CH_2Cl_2** and **(ClL1Pd)$_2$·2CH_2Cl_2**.

Parameter	BrL0Pd·CH_2Cl_2	(ClL1Pd)$_2$·2CH_2Cl_2
Empirical formula	$C_{22}H_{13}Br_2Cl_3N_2PdS_2$	$C_{52}H_{40}Cl_8N_4O_4Pd_2S_4$
Formula weight	742.03	1409.52
Temperature	302(2) K	130(2) K
Wavelength	0.71073 Å	1.5417 Å
Crystal system	Monoclinic	Triclinic
space group	P2(1)/c	P-1
Unit cell dimensions	a = 10.0437(4) Å α= 90°	a = 9.1706(4) Å α= 77.438(2)°
	b = 17.3496(7) Å β= 109.3250(10)°	b = 10.5573(5) Å β= 76.466(2)°
	c = 14.6181(6) Å γ= 90°	c = 14.9910(7) Å γ= 71.907(2)°
Volume	2403.74(17) Å^3	1324.73(11) Å^3
Z	4	1
Density (calculated)	2.050 Mg/m^3	1.767 Mg/m^3
Absorption coefficient	4.619 mm^{-1}	11.082 mm^{-1}
F(000)	1432	704
Crystal size	0.80 x 0.35 x 0.35 mm	0.330 x 0.060 x 0.020 mm
Theta range for data collection	2.953 to 26.320°	3.070 to 66.640°
Limiting indices	-12<=h<=12, -21<=k<=15, -18<=l<=18	-10<=h<=10, -12<=k<=12, -17<=l<=17
Reflections collected	18896	17425
Independent reflections	4872 [R(int) = 0.0208]	4608 [R(int) = 0.0507]
Completeness to theta = 25.242°	99.7 %	98.4%
Absorption correction	Semi-empirical from equivalents	Semi-empirical from equivalents
Refinement method	Full-matrix least-squares on F^2	Full-matrix least-squares on F^2
Data / restraints / parameters	4872 / 0 / 289	4608 / 0 / 336
Goodness-of-fit on F2	1.030	1.072
Final R indices [I>2sigma(I)]	R1 = 0.0264, wR2 = 0.0632	R1 = 0.0440, wR2 = 0.1247
R indices (all data)	R1 = 0.0323, wR2 = 0.0665	R1 = 0.0450, wR2 = 0.1257
Extinction coefficient	n/a	n/a
CCDC No.	1914874	1914875

Computational Methods:

The initial geometries of the optimized monomer and quinoid dimer were directly obtained from the X-ray crystal structure, while the initial geometry of the aromatic dimer was acquired by modifying the bond length of quinoid dimers' crystal structure and planar conformation was employed. The calculations of absorption spectra were performed by TDDFT method at the same calculation level of (Hybrid Function/LANL2DZ for Pd/6-31g (d, p) for other atoms/PCM (dichloromethane)).

Calculations of **ClL1Pd** based monomer, aromatic and quinoid dimer were performed with Density Functional Theory (DFT) using the Gaussian09 program package[6]. Different hybrid function such as ωB97X, PBE0, B3LYP and M06 were employed for the geometry optimizations, frequency calculations and TDDFT calculations, where the 6-31G (d, p) basis set[7,8] was used for hydrogen, carbon, nitrogen, sulfur and chlorine atoms, and the valence atomic orbitals of palladium were described by LANL2DZ basis set and the effective core potentials (ECPs) proposed by Hay and Wadt[9,10] were employed. Solvent effects were taken into account using the polarizable continuum model (PCM) with dichloromethane as solvent. The spectra calculated were compared with the experimental spectrum (Figure S10), which shows the spectra from hybrid function PBE0 matched well with the experimental data. Thus the following calculations were conducted on the basis of hybrid function PBE0.

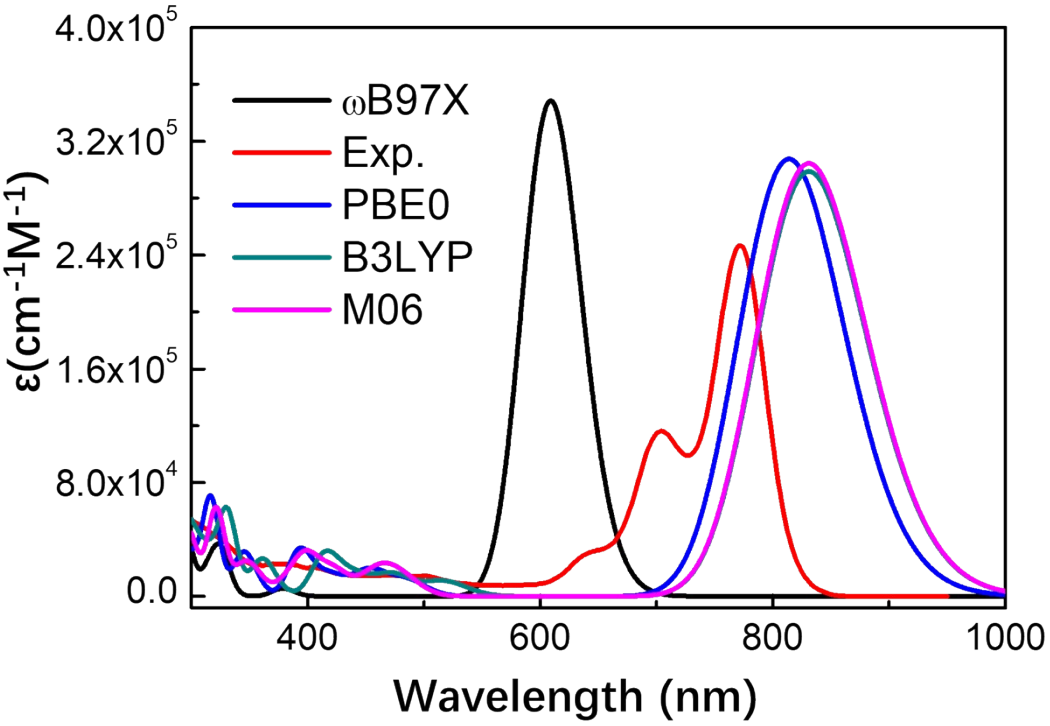

Figure S10. Comparison of experimental absorption spectra with calculated spectra based on different hybrid functions.

Table S5. Selected excitation wavelengths and oscillator strengths of **(ClL1Pd)$_2$**

Excited State	Excitation Wavelength (nm)	Excitation Wavelength (eV)	Oscillator Strength, *f*	Excited State	CI Coefficient
1	813.96	1.5232	2.2799	MO282 -> MO283	0.70535
2	503.54	2.4623	0.0000	MO282 -> MO284	0.69283
3	485.21	2.5552	0.0842	MO282 -> MO285	0.69819
4	477.21	2.5981	0.0000	MO271 -> MO283 MO281 -> MO283	0.12335 0.66996
5	461.05	2.6892	0.0000	MO282 -> MO286	0.68550

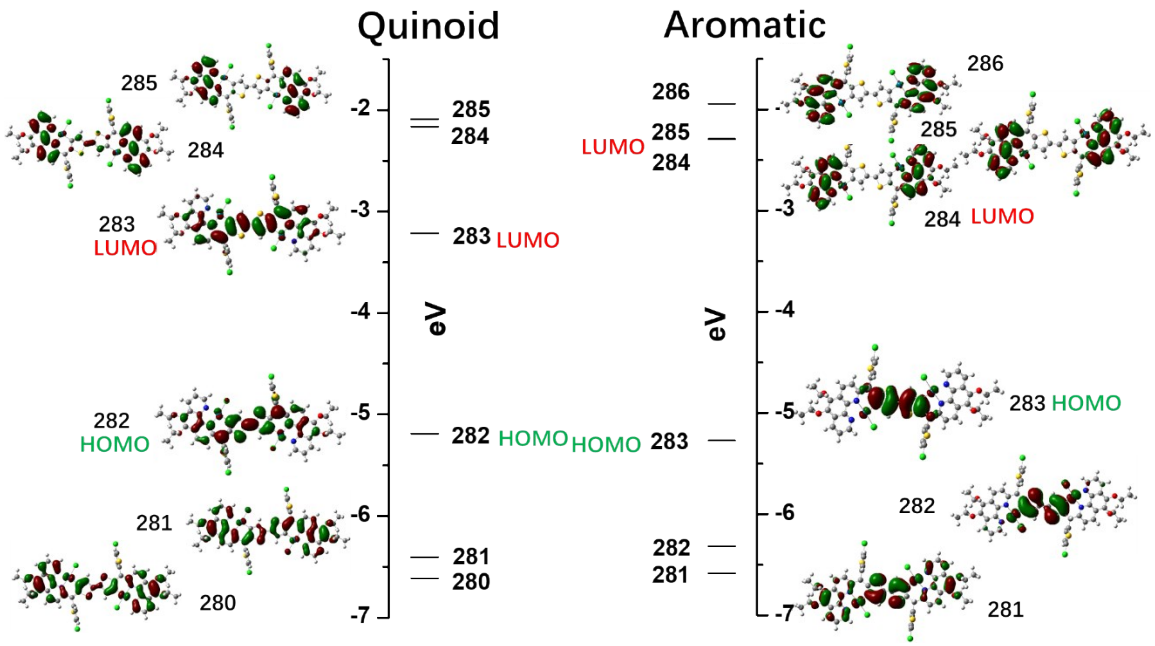

Figure S11. Frontier molecular orbital (FMO) results of aromatic and quinoid dimer.

4. NMR spectra

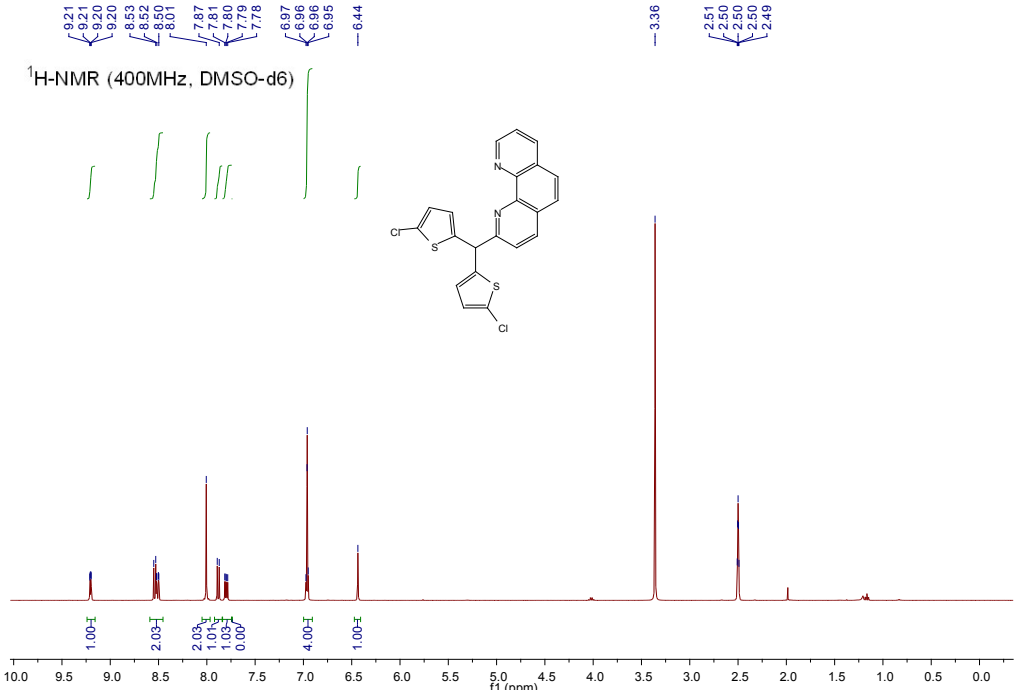

Figure S12. ^{1}H-NMR spectrum of ligand **ClL0**.

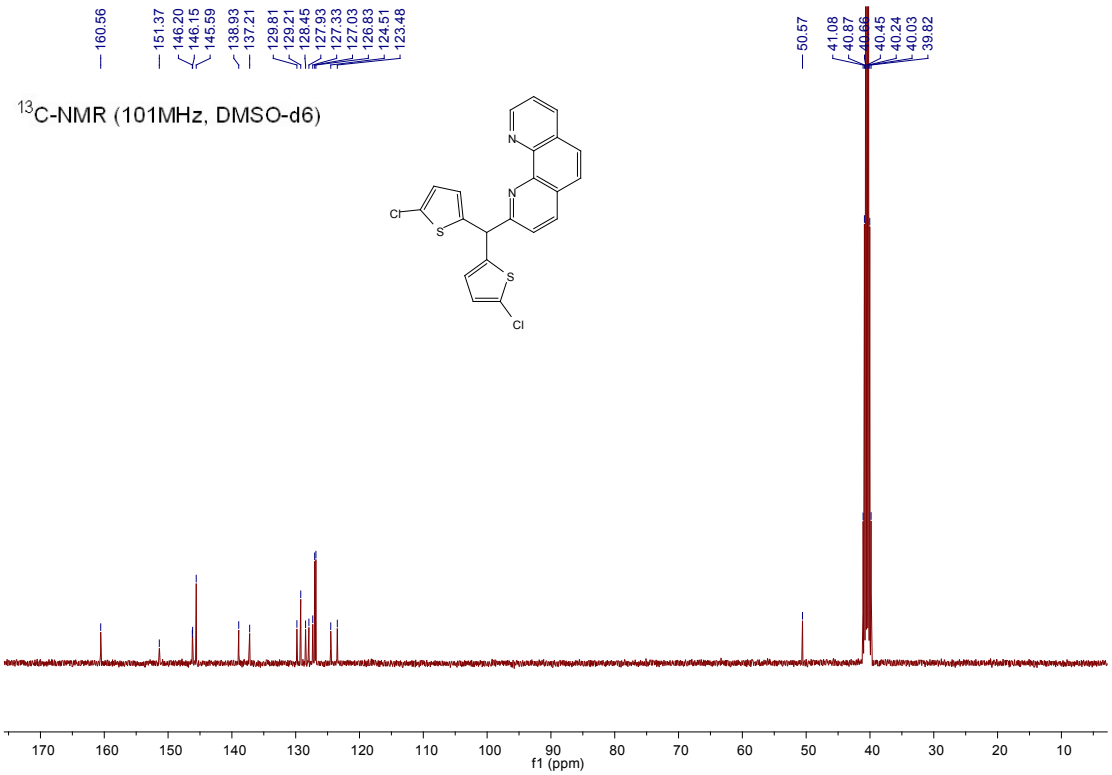

Figure S13. ^{13}C-NMR spectrum of ligand **ClL0**.

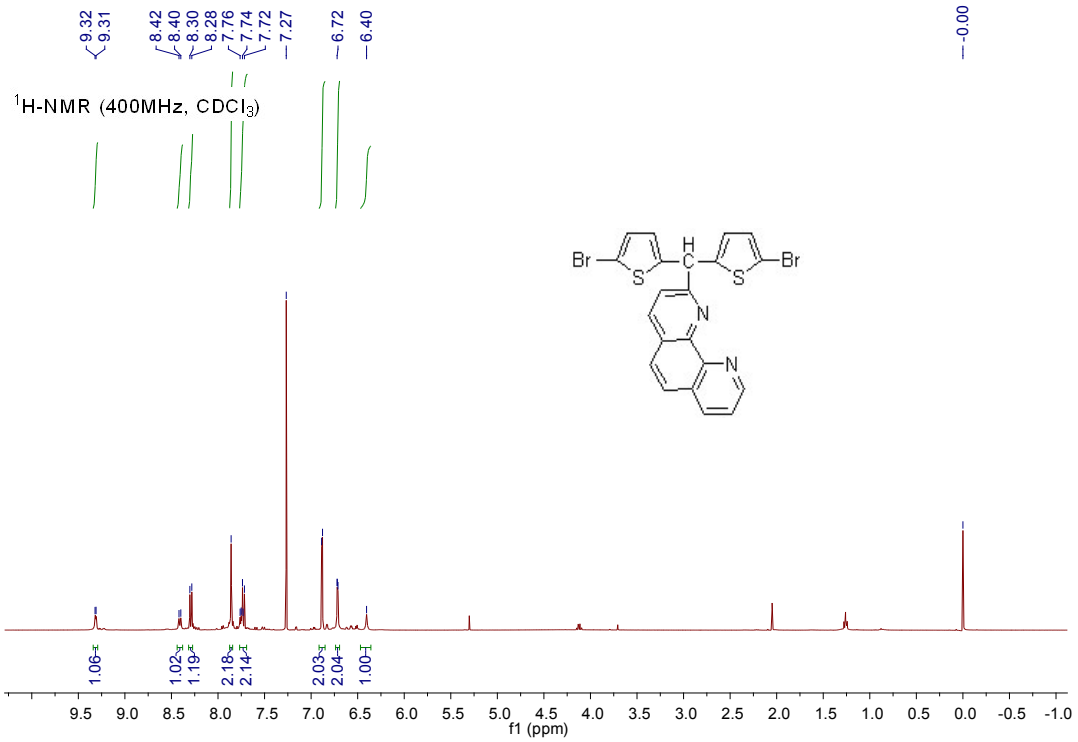

Figure S14. ^{1}H-NMR spectrum of ligand **BrL0**.

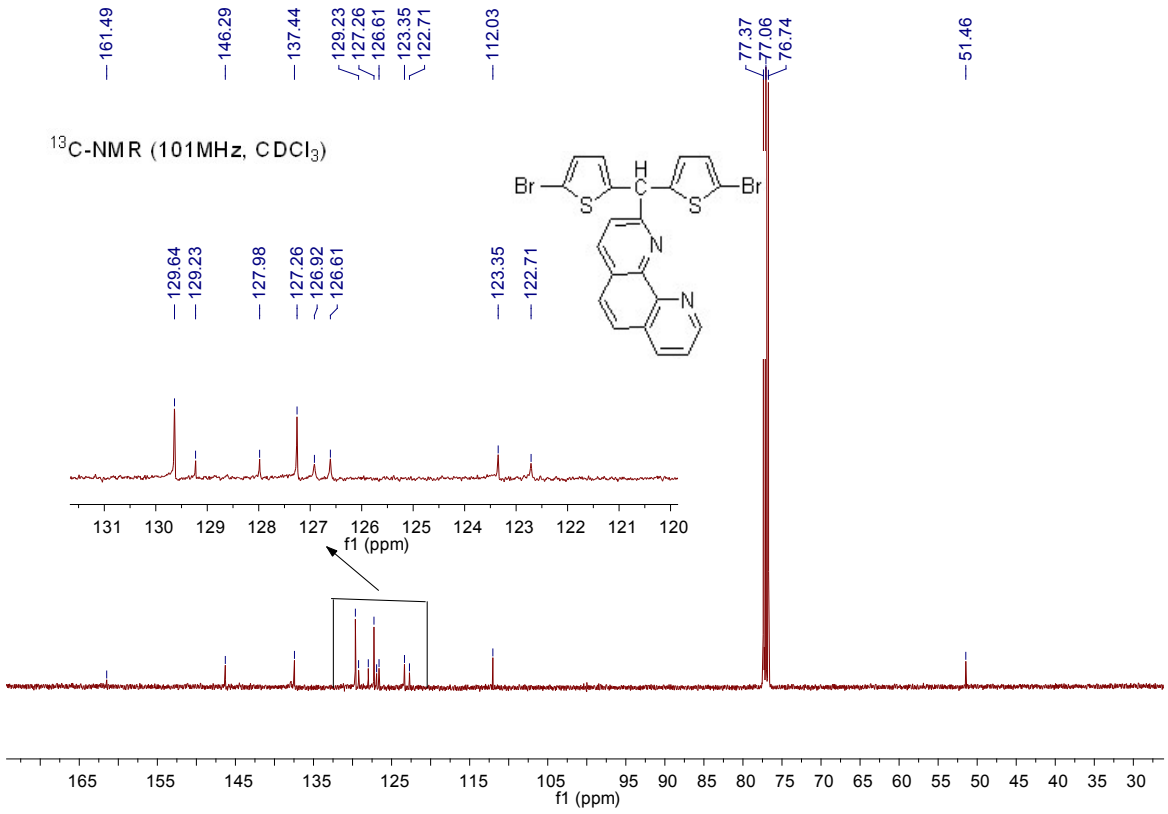

Figure S15. ^{13}C-NMR spectrum of ligand **BrL0**.

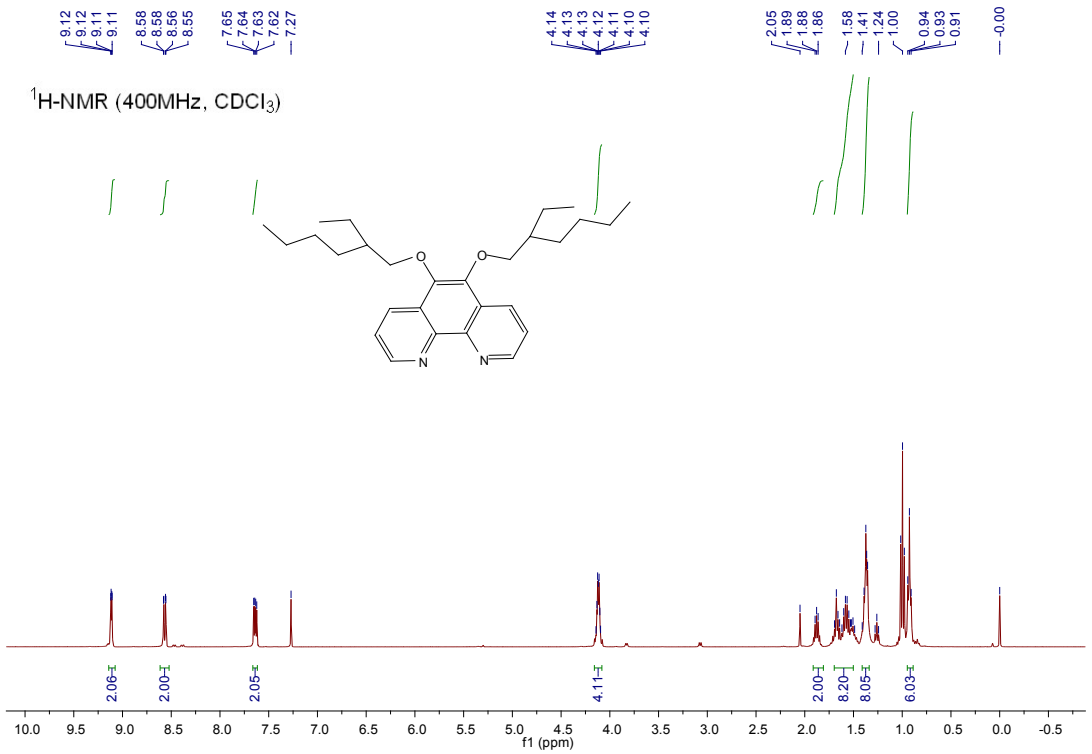

Figure S16. ^{1}H-NMR spectrum of ligand **a1**.

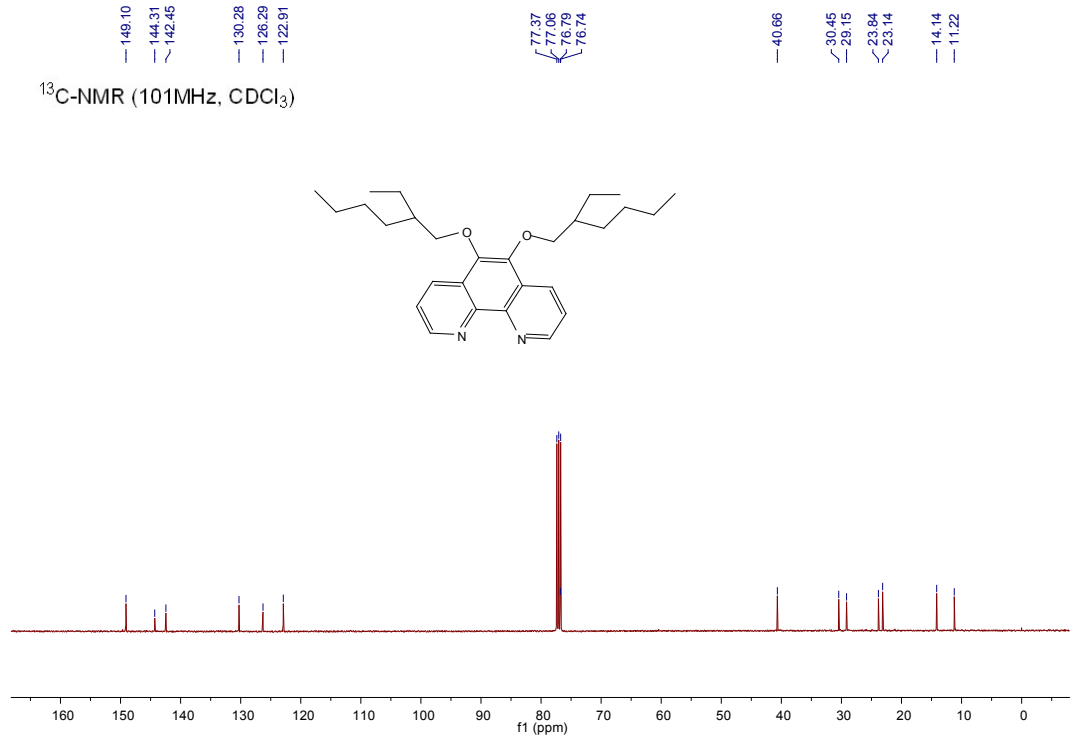

Figure S17. ^{13}C-NMR spectrum of ligand **a1**.

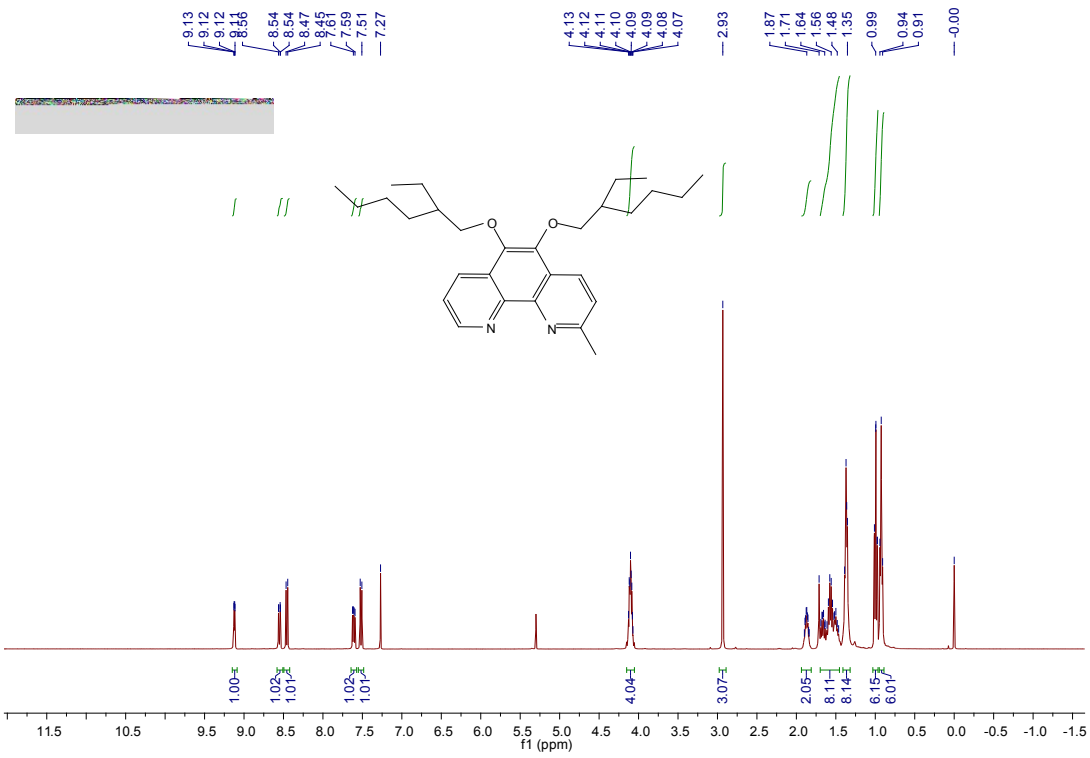

Figure S18. ^{1}H-NMR spectrum of ligand **b1**.

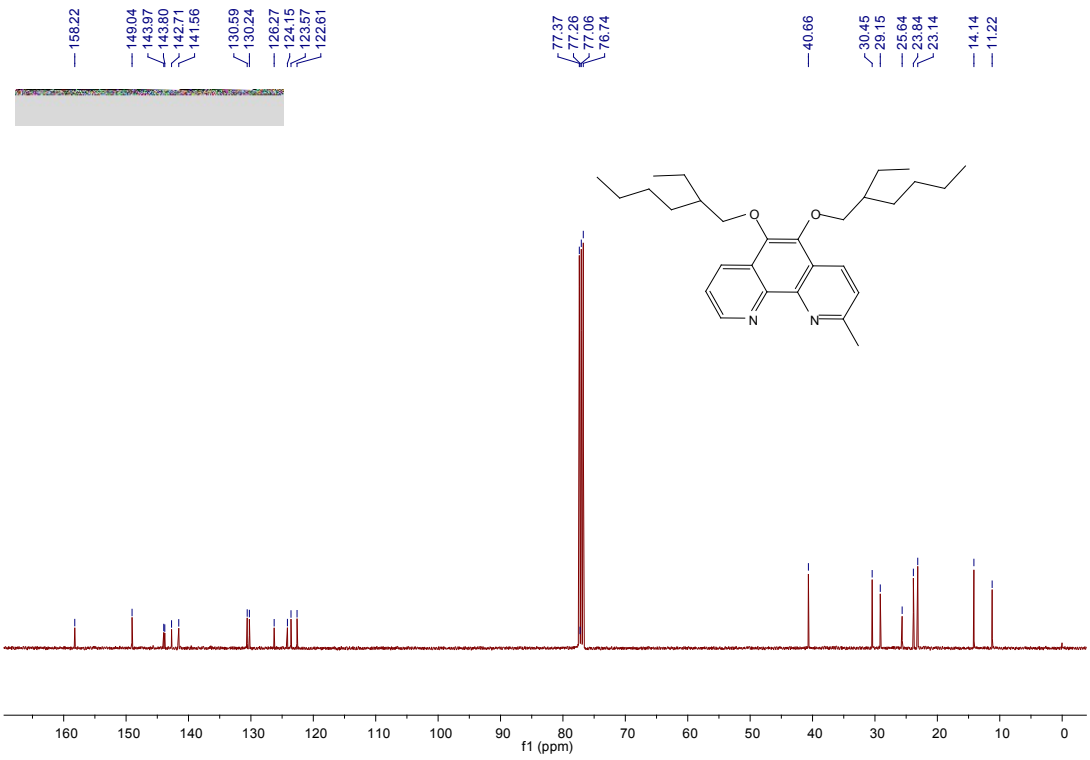

Figure S19. ^{13}C-NMR spectrum of ligand **b1**.

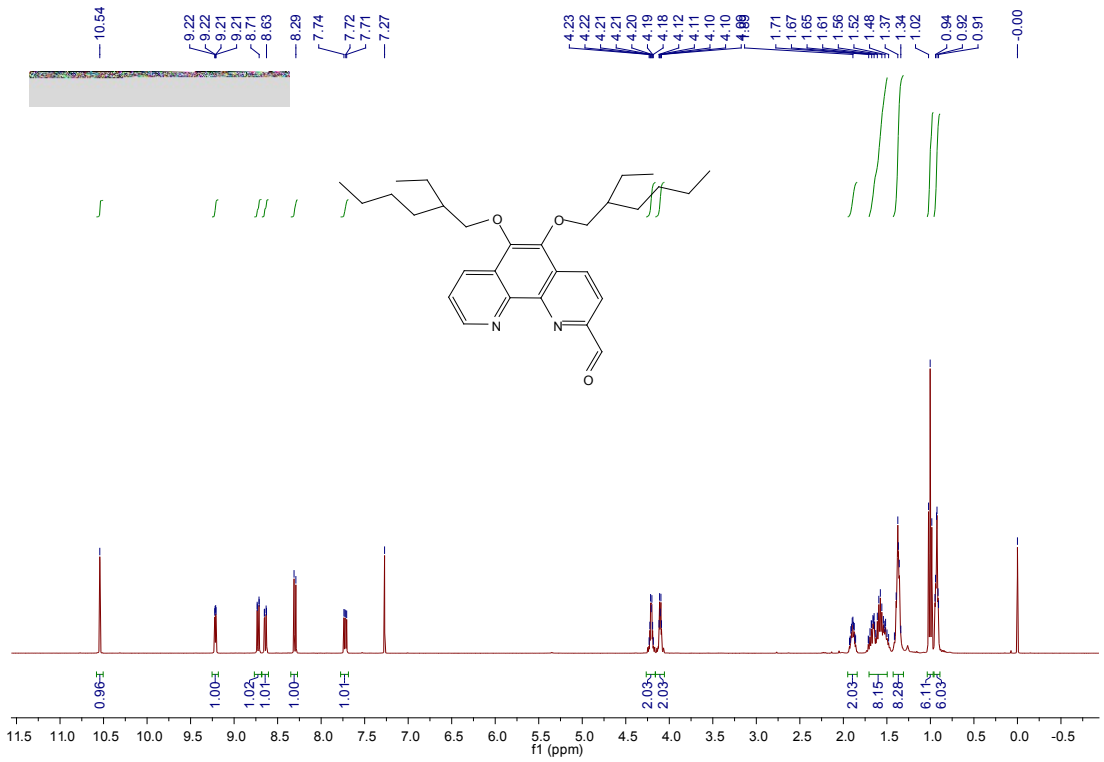

Figure S20. ^{1}H-NMR spectrum of ligand **c1**.

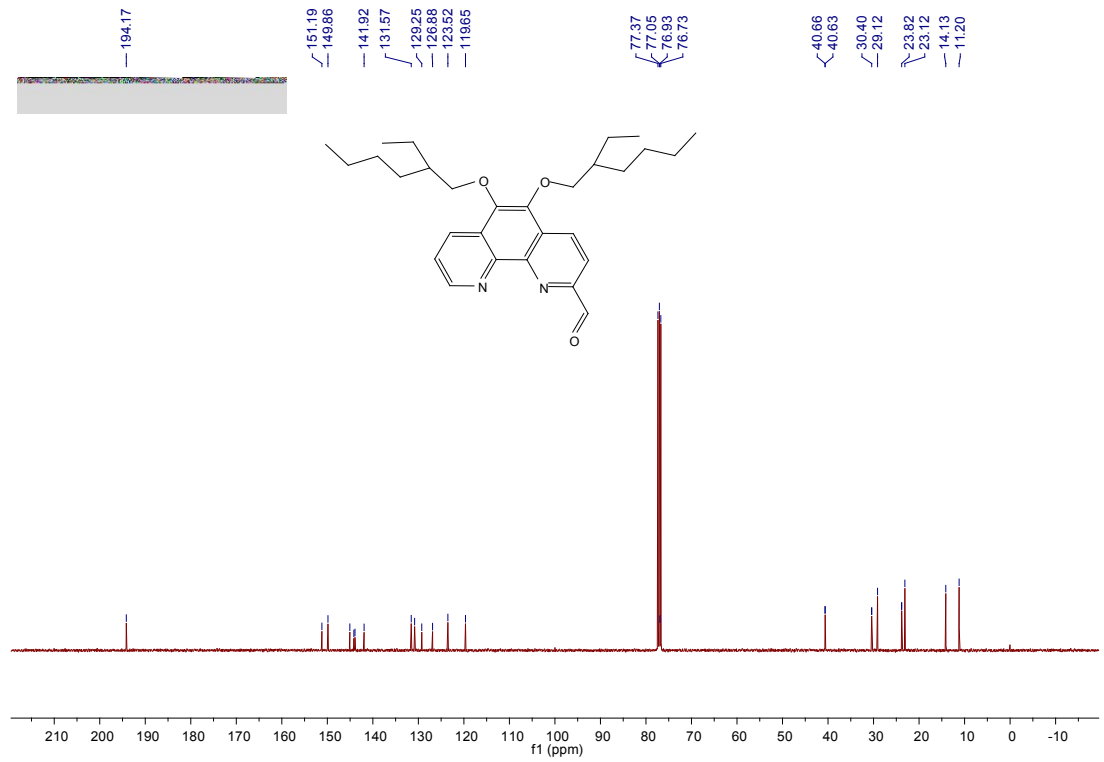

Figure S21. ^{13}C-NMR spectrum of ligand **c1**.

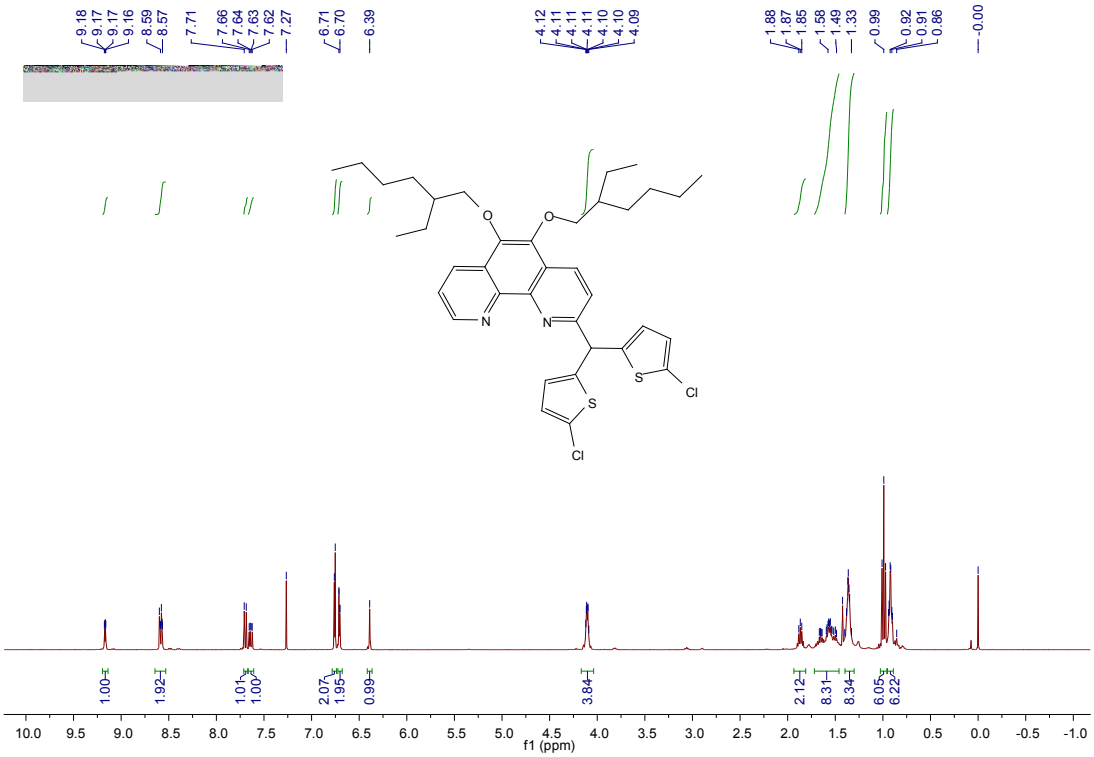

Figure S22. ^{1}H-NMR spectrum of ligand **ClL2**.

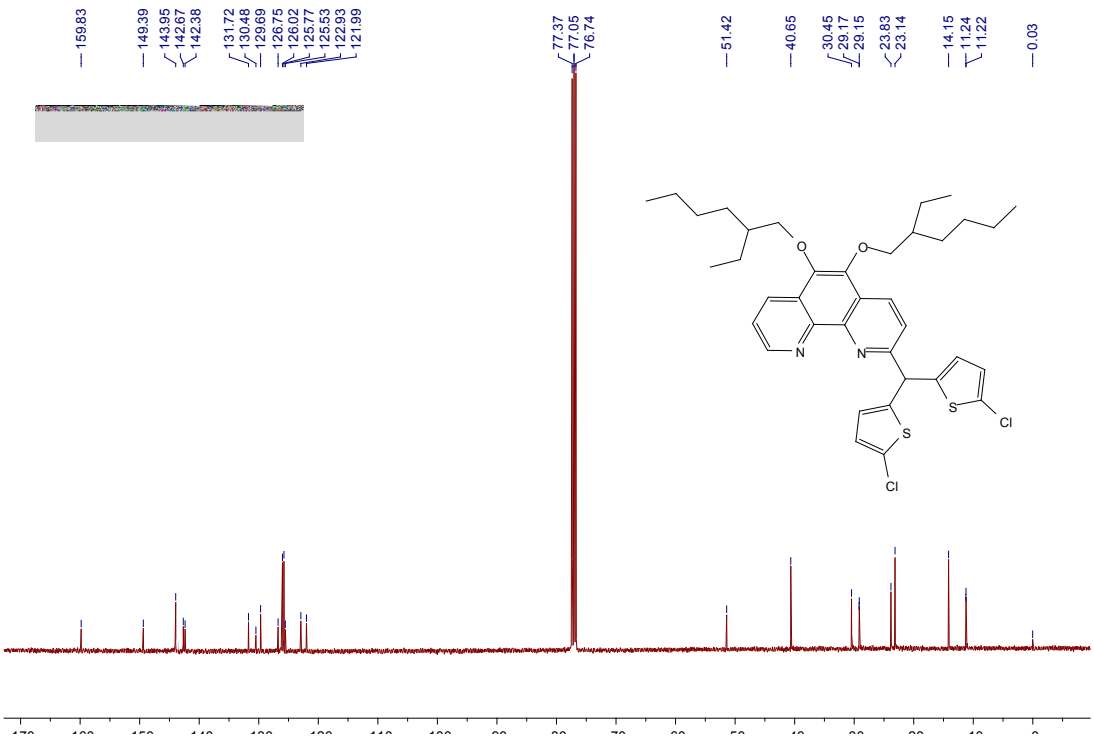

Figure S23. ^{13}C-NMR spectrum of ligand **ClL2**.

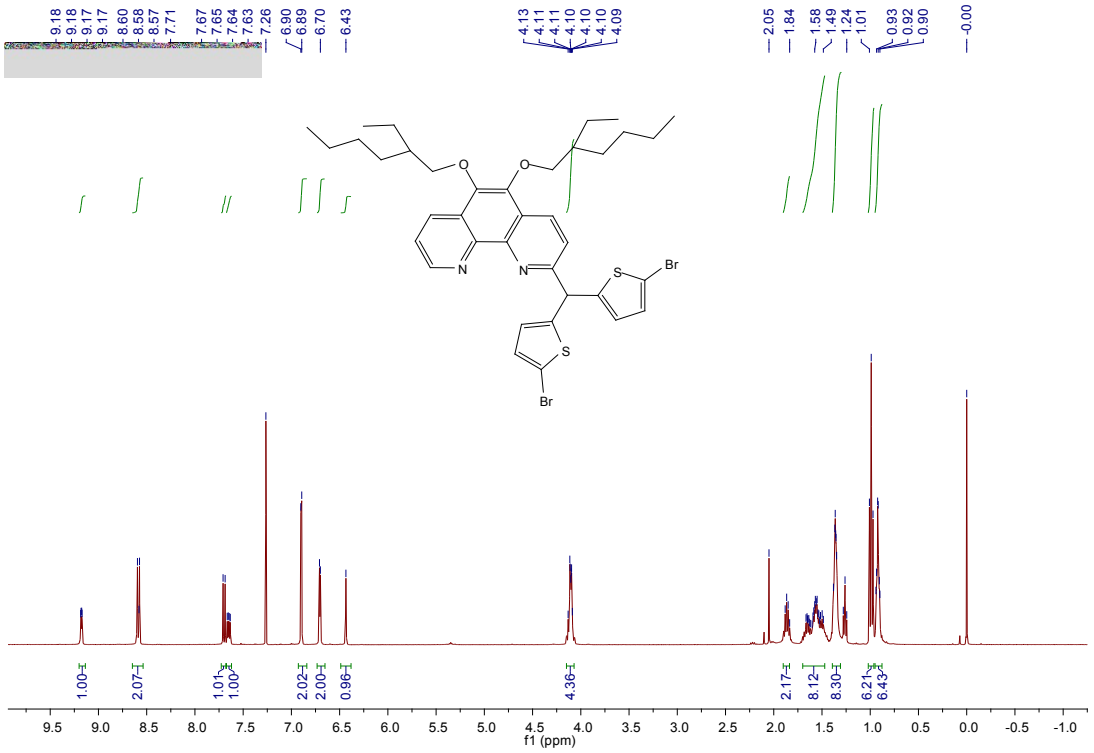

Figure S24. Figure/Scheme Caption.

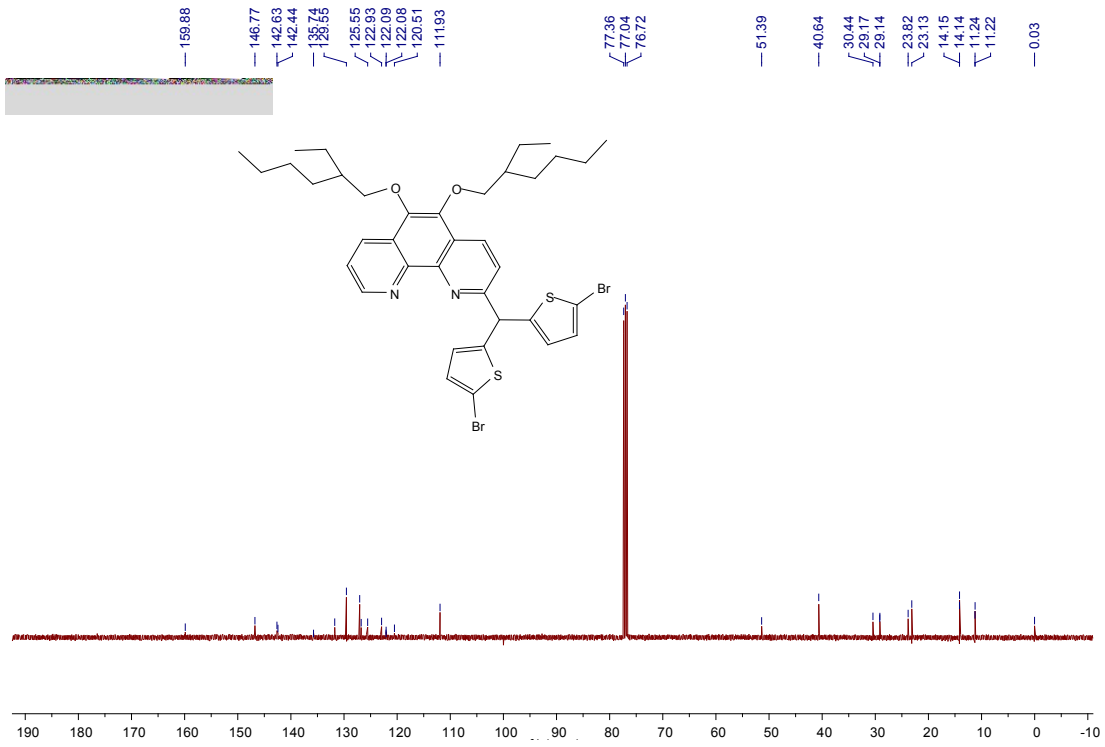

Figure S25. ^{13}C-NMR spectrum of ligand **BrL2**.

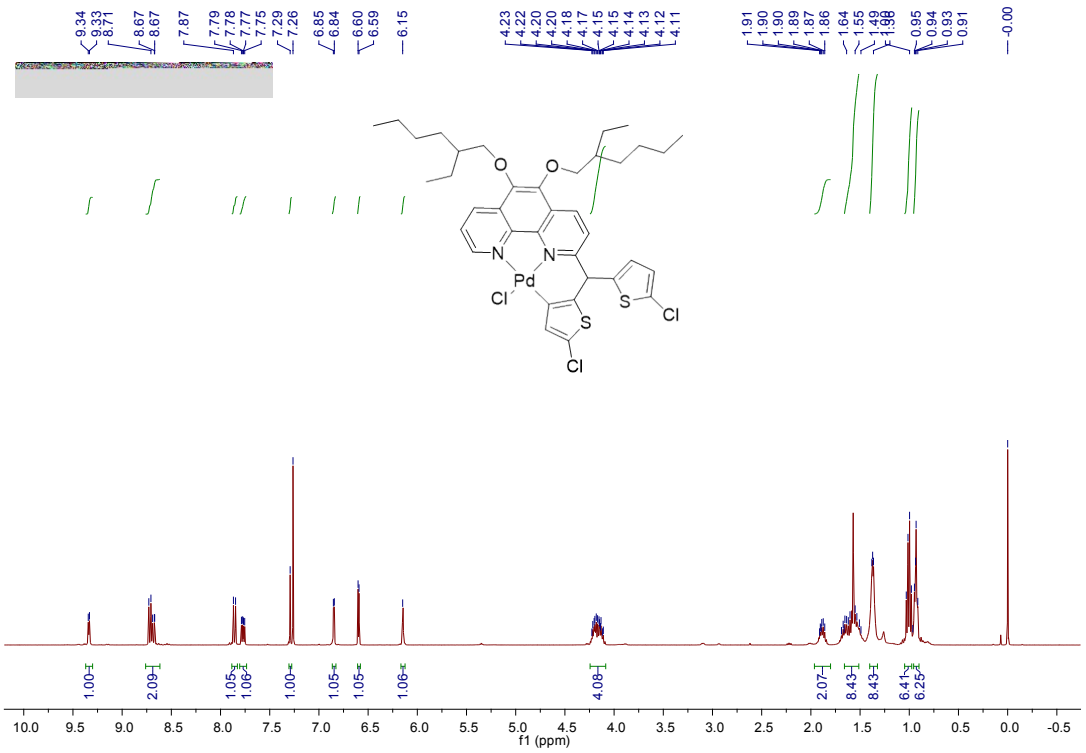

Figure S26. ^{1}H-NMR spectrum of ligand **ClL2Pd**.

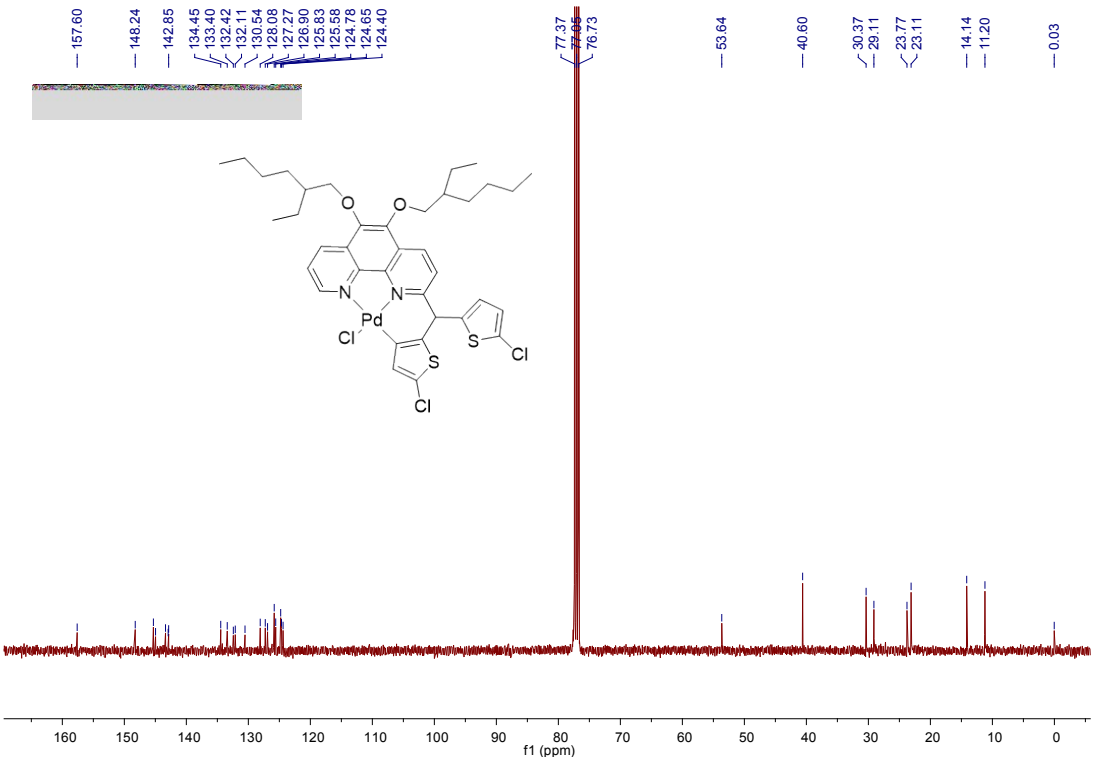

Figure S27. ^{13}C-NMR spectrum of ligand **ClL2Pd**

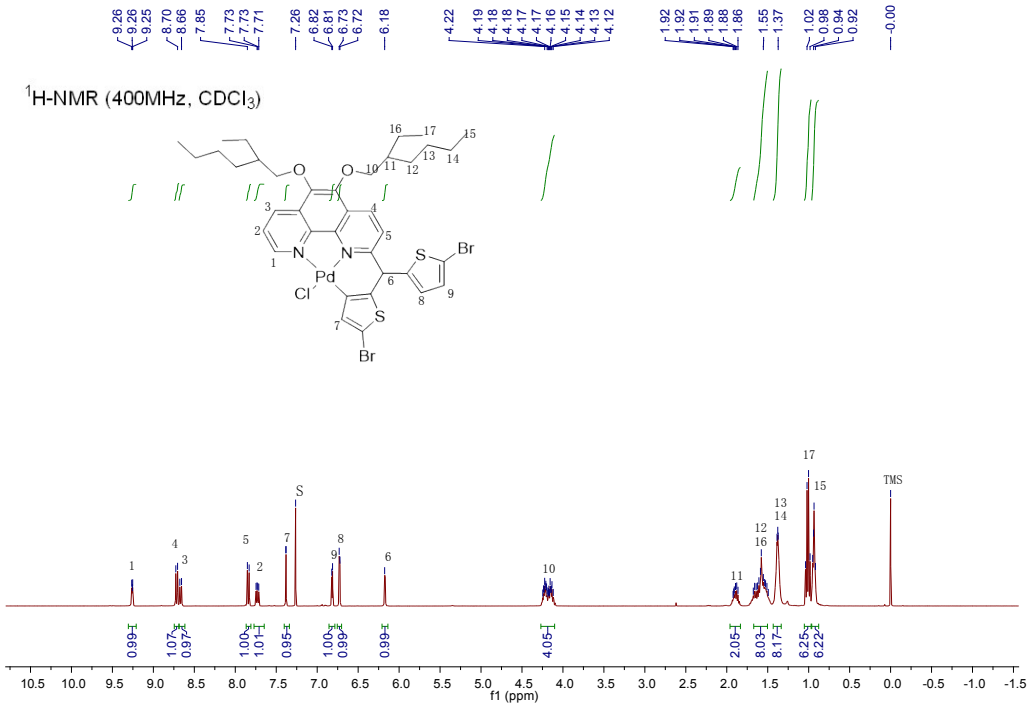

Figure S28. ^{1}H-NMR spectrum of ligand **BrL2Pd**.

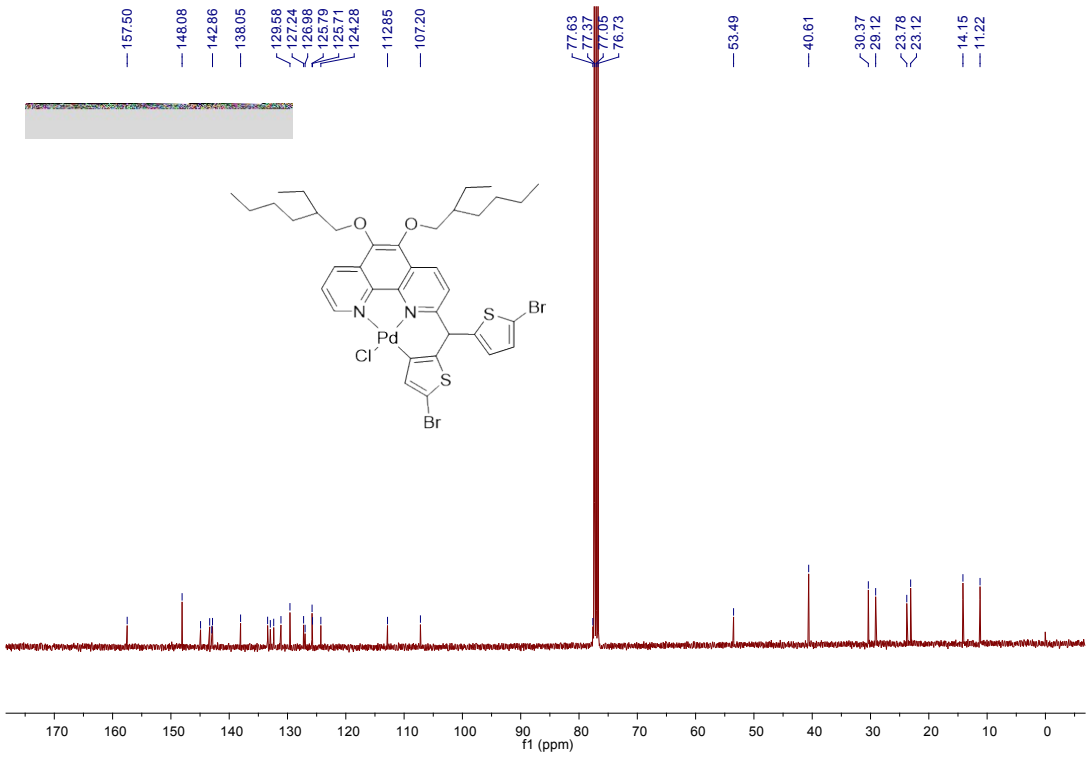

Figure S29. ^{13}C-NMR spectrum of ligand **BrL2Pd**..

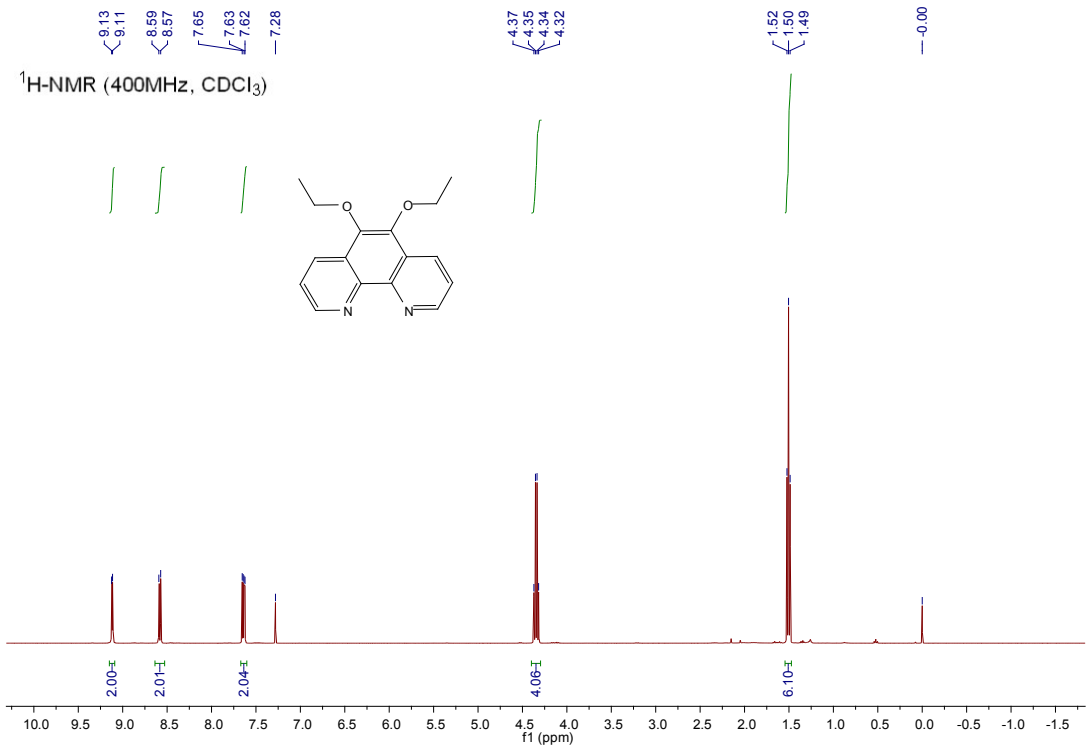

Figure S30. ^{1}H-NMR spectrum of ligand **a2**.

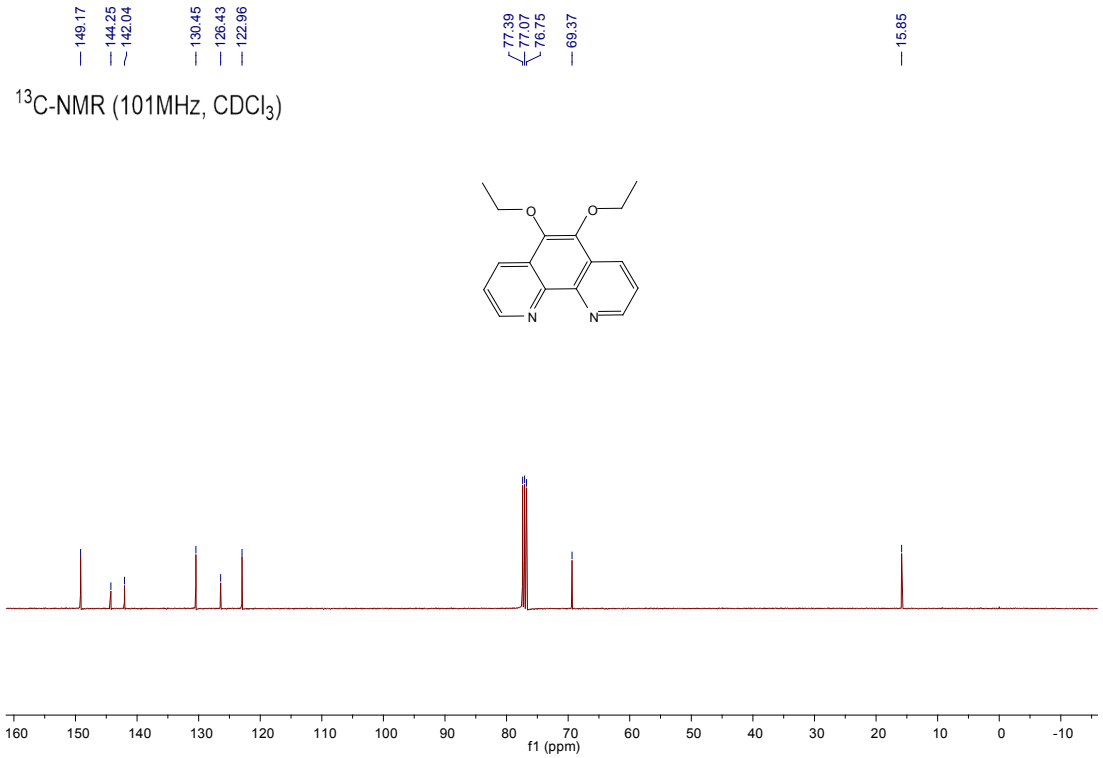

Figure S31. ^{13}C-NMR spectrum of ligand **a2**.

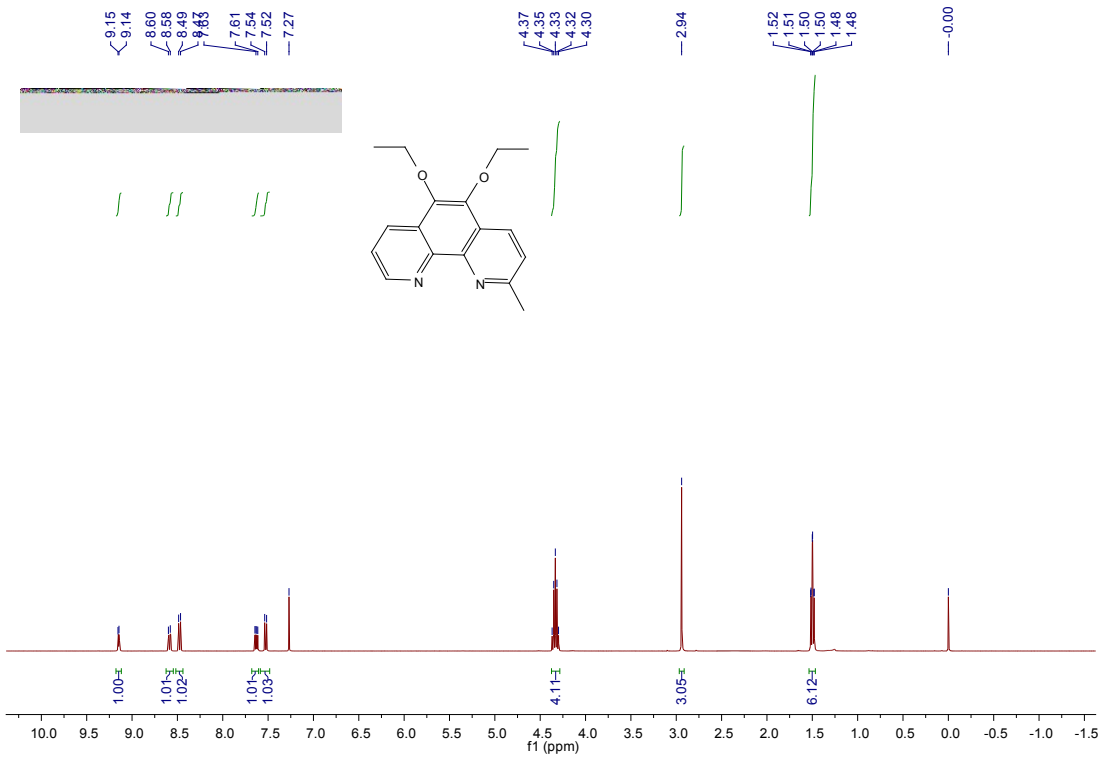

Figure S32. ^{1}H-NMR spectrum of ligand **b2**.

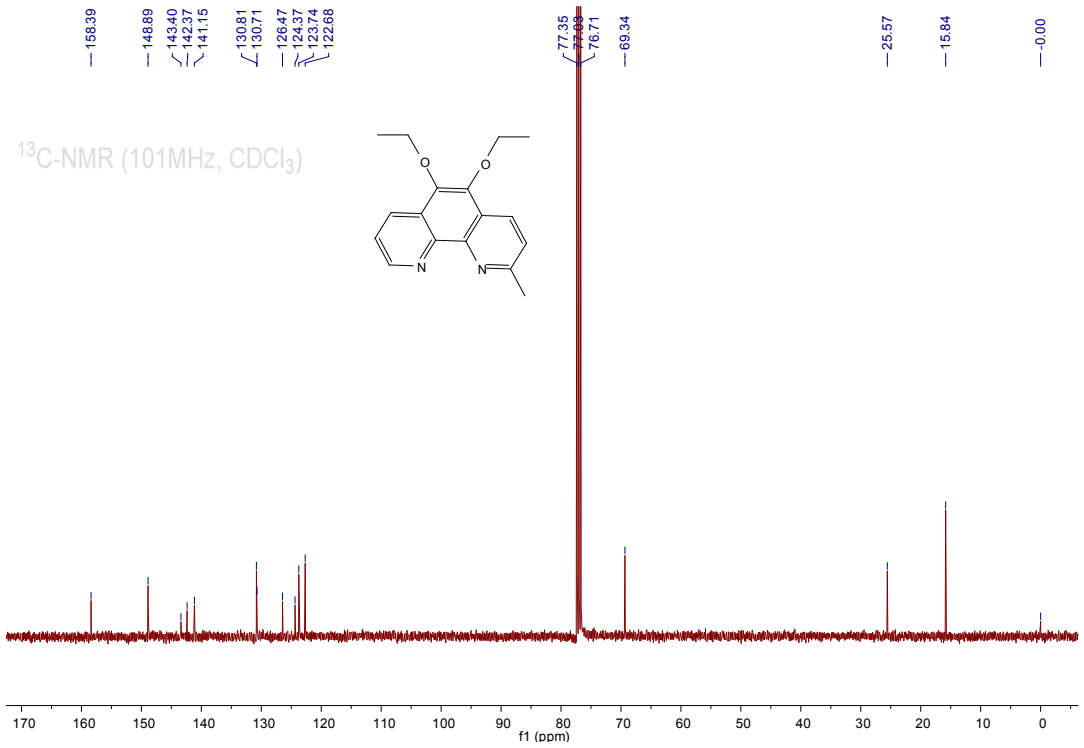

Figure S33. ^{13}C-NMR spectrum of ligand **b2**.

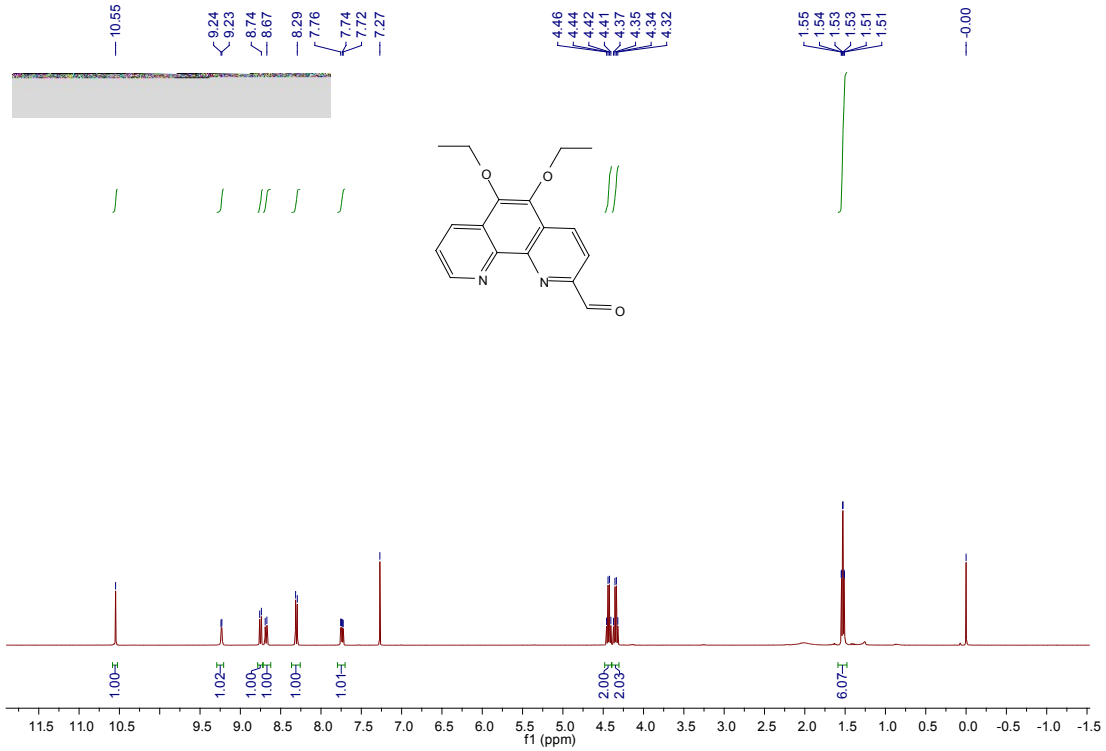

Figure S34. ^{1}H-NMR spectrum of ligand **c2**.

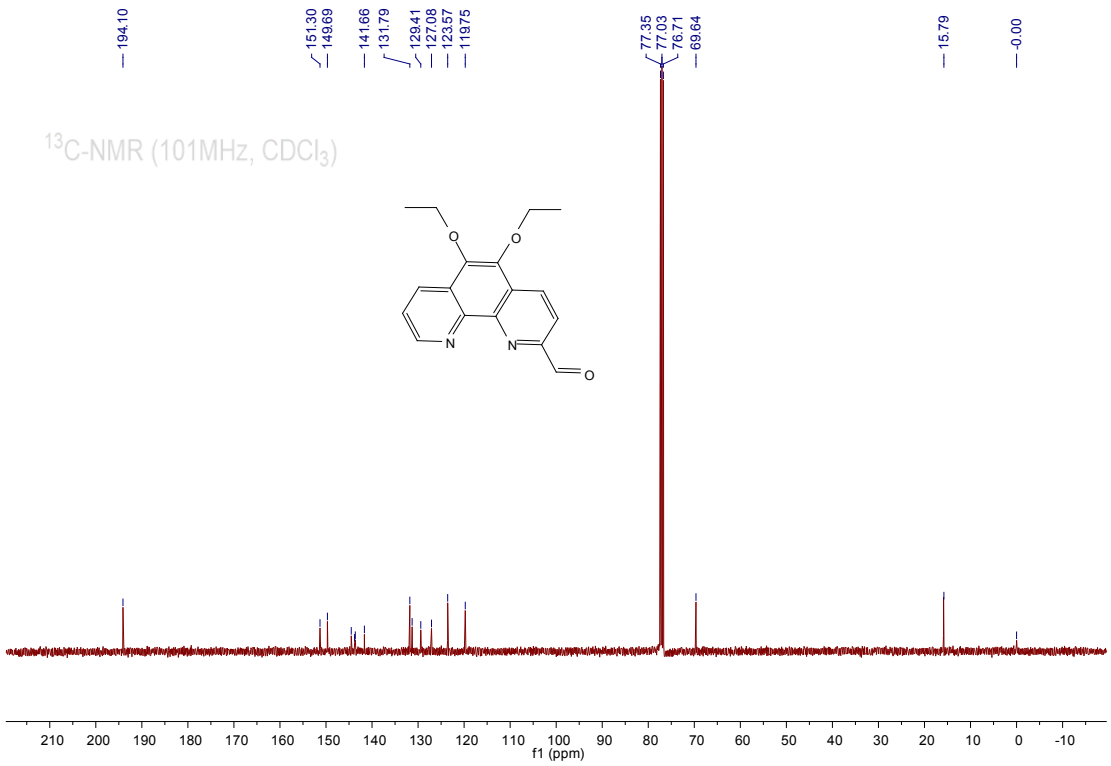

Figure S35. ^{13}C-NMR spectrum of ligand **c2**.

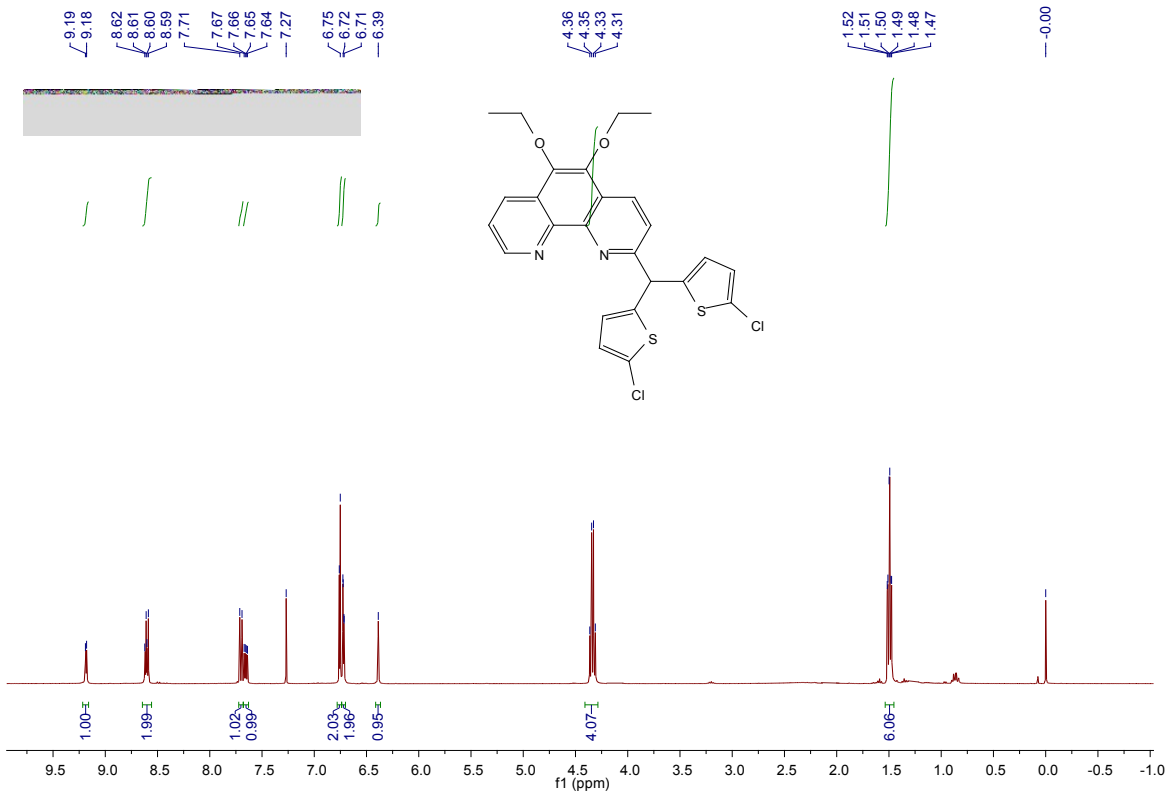

Figure S36. ^{1}H-NMR spectrum of ligand **ClL1**.

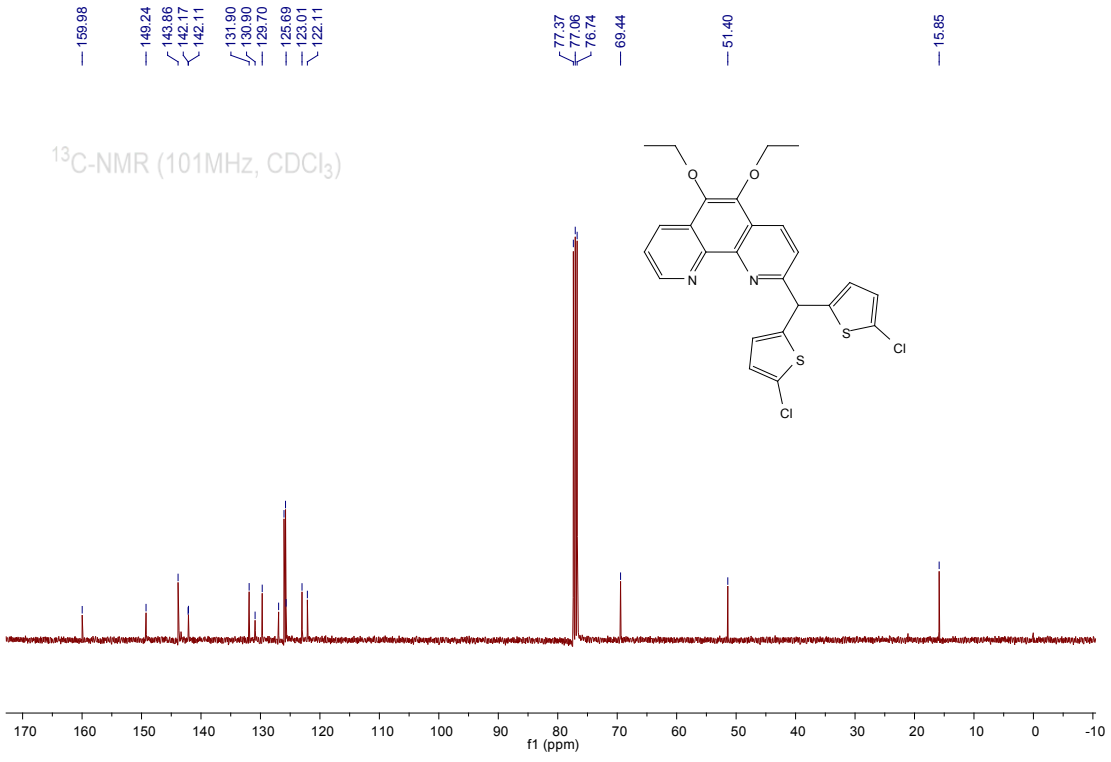

Figure S37. ^{13}C-NMR spectrum of ligand **ClL1**..

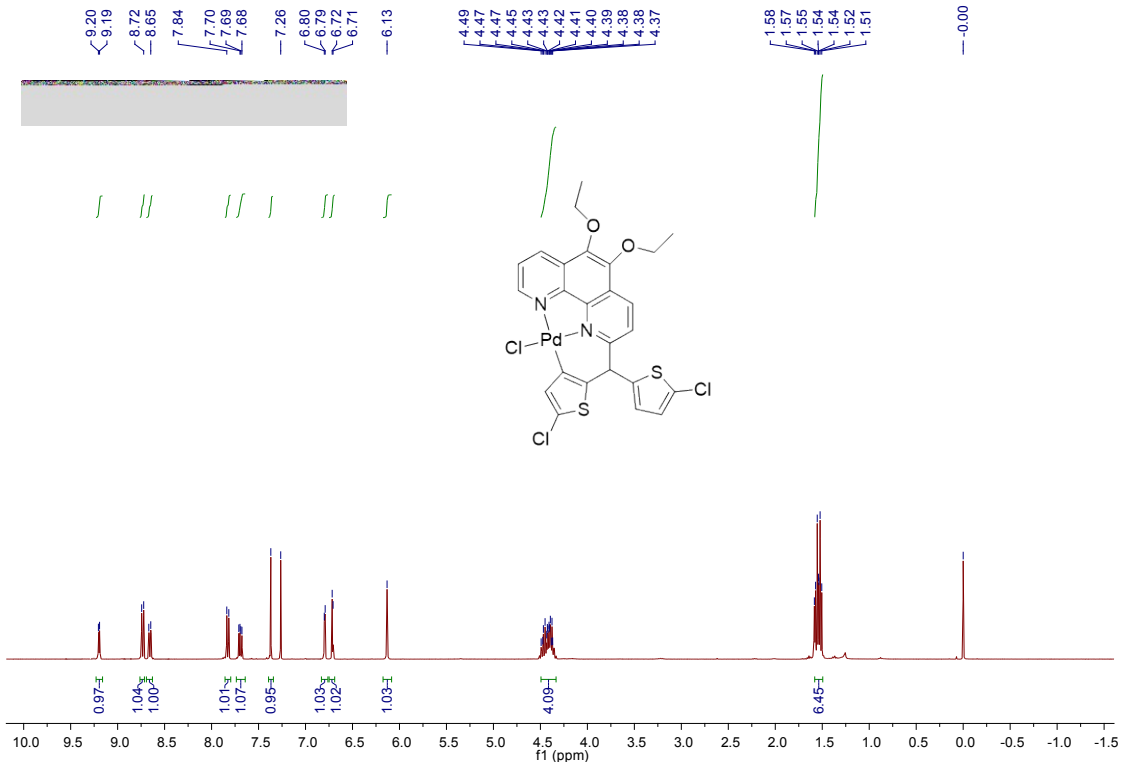

Figure S38. ^{1}H-NMR spectrum of ligand **ClL1Pd**.

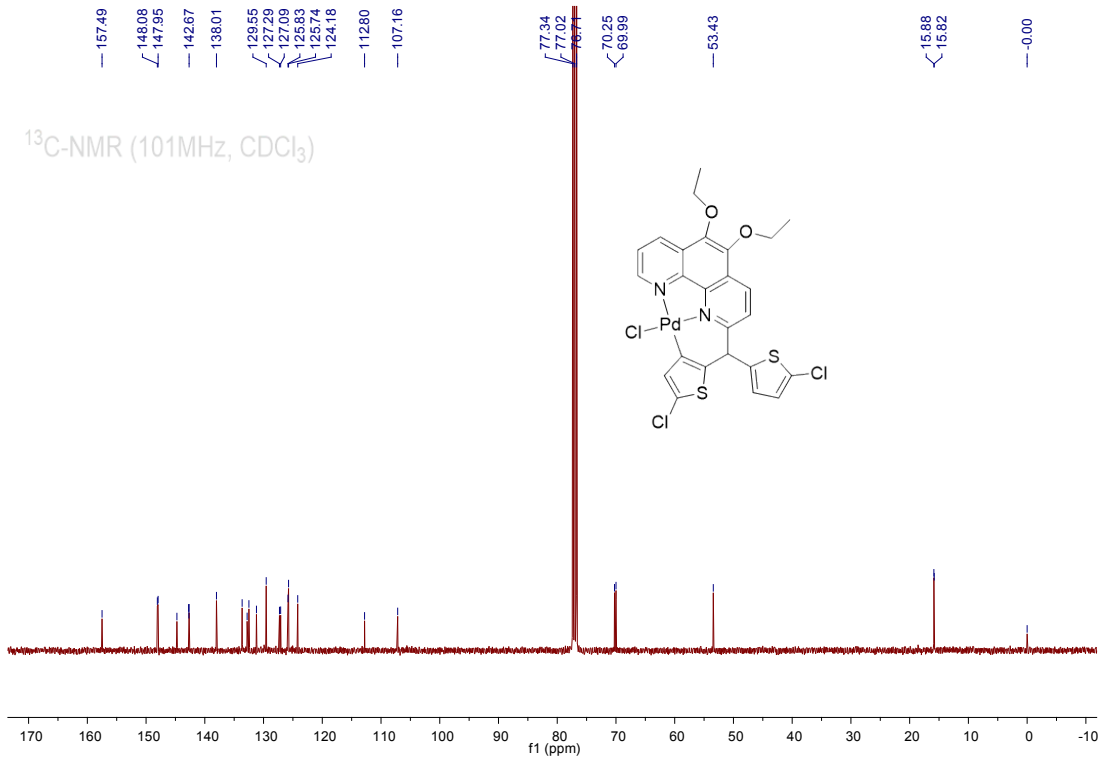

Figure S39. ^{13}C-NMR spectrum of ligand **ClL1Pd**.

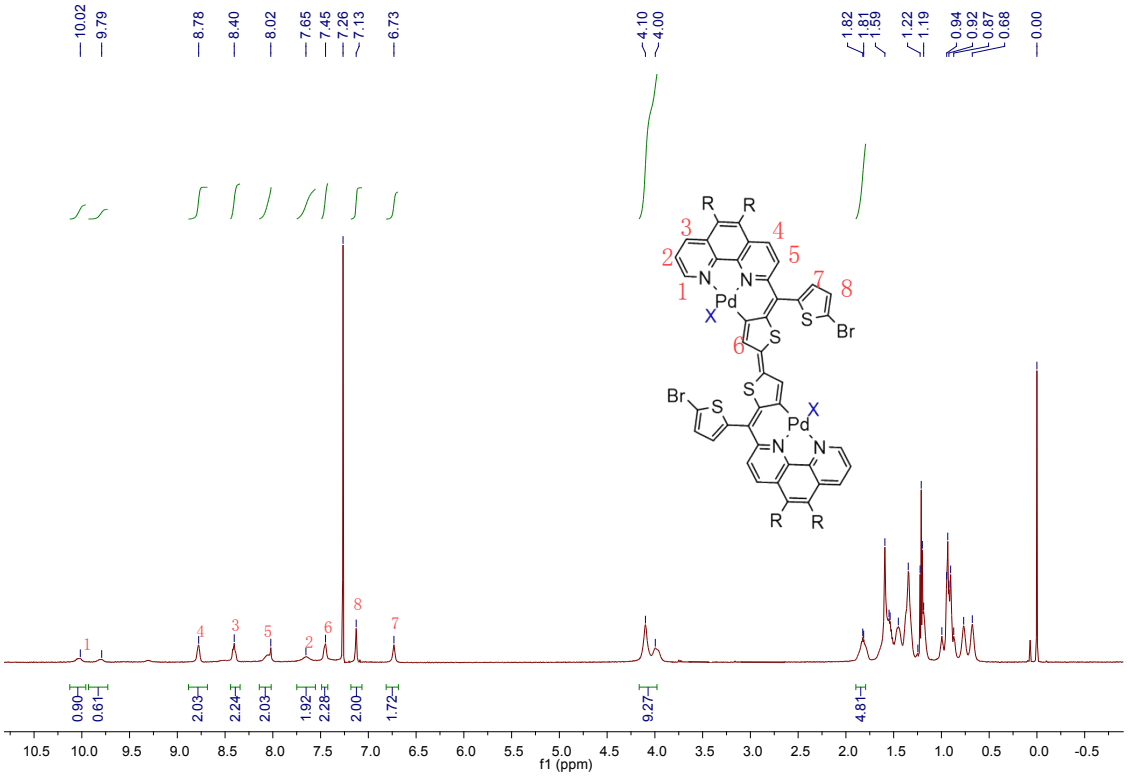

Figure S40. ^{1}H-NMR spectrum of ligand **(BrL2Pd)$_2$**, the divided signals of H1 was ascribed to the different X (9.79 ppm for Cl and 10.02 ppm for Br).

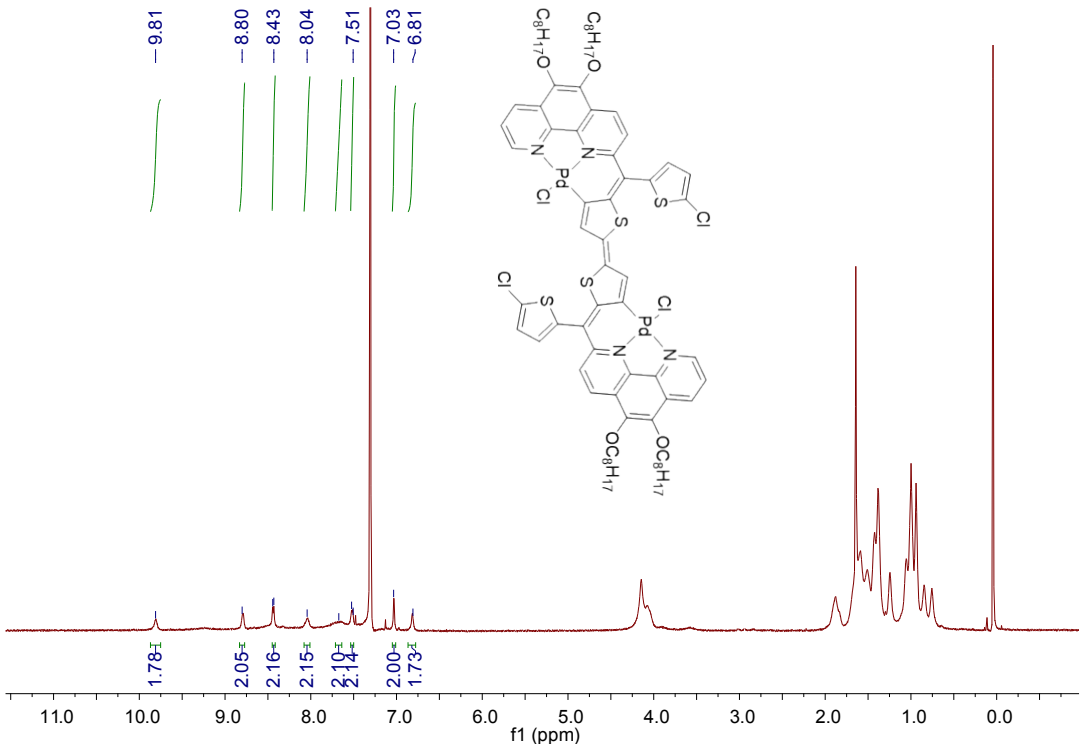

Figure S41. ^{1}H-NMR spectrum of ligand **$(ClL2Pd)_2$**.

5. References

[1] M. Zhang, R. Gao, X. Hao and W. Sun, *J. Organomet. Chem.*, 2008, **693**, 3867-3877..

[2] M. G. Schwab, M. Takase, A. Mavrinsky, W. Pisula, X. Feng, J. A. Gámez, W. Thiel, K. S. Mali, S. de Feyter and K. Müllen, *Chem. - Eur. J.*, 2015, **21**, 8426-8434.

[3] M. Li, B. W. Chu, N. Zhu and V. W. Yam, *Inorg. Chem*., 2007, **46**, 720-733.

[4] Q. Luo, K. Peng, J. Zhang and J. Xia, *Organometallics*, 2019, **38**, 647-653.

[5] C. M. Cardona, W. Li, A. E. Kaifer, D. Stockdale and G. C. Bazan, *Adv. Mater.*, 2011, **23**, 2367-2371.

[6] Gaussian 09, Revision D.01, M. J. Frisch, G. W. Trucks, H. B. Schlegel, G. E. Scuseria, M. A. Robb, J. R. Cheeseman, G. Scalmani, V. Barone, G. A. Petersson, H. Nakatsuji, X. Li, M. Caricato, A. Marenich, J. Bloino, B. G. Janesko, R. Gomperts, B. Mennucci, H. P. Hratchian, J. V. Ortiz, A. F. Izmaylov, J. L. Sonnenberg, D. Williams-Young, F. Ding, F. Lipparini, F. Egidi, J. Goings, B. Peng, A. Petrone, T.

Henderson, D. Ranasinghe, V. G. Zakrzewski, J. Gao, N. Rega, G. Zheng, W. Liang, M. Hada, M. Ehara, K. Toyota, R. Fukuda, J. Hasegawa, M. Ishida, T. Nakajima, Y. Honda, O. Kitao, H. Nakai, T. Vreven, K. Throssell, J. A. Montgomery, Jr., J. E. Peralta, F. Ogliaro, M. Bearpark, J. J. Heyd, E. Brothers, K. N. Kudin, V. N. Staroverov, T. Keith, R. Kobayashi, J. Normand, K. Raghavachari, A. Rendell, J. C. Burant, S. S. Iyengar, J. Tomasi, M. Cossi, J. M. Millam, M. Klene, C. Adamo, R. Cammi, J. W. Ochterski, R. L. Martin, K. Morokuma, O. Farkas, J. B. Foresman and D. J. Fox, *Gaussian, Inc., Wallingford CT*, **2013**.

[7] M. J. Frisch, J. A. Pople and J. S. Binkley, *J. Chem. Phys*. **1984**, *80*, 3265-3269.

[8] L. Radom, P. C. Hariharan, J. A. Pople and P. V. R. Schleyer, *J. Am. Chem. Soc.*, 1973, **95**, 6531-6544.

[9] W. R. Wadt and P. J. Hay, *J. Chem. Phys.*, 1985, **82**, 284-298

[10] P. J. Hay and W. R. Wadt, *J. Chem. Phys.*, 1985, **82**, 299-310